

# Role of Xanthophylls in Light Harvesting in Green Plants: A Spectroscopic Investigation of Mutant LHCII and Lhcb Pigment–Protein Complexes

Marcel Fuciman,<sup>†</sup> Miriam M. Enriquez,<sup>†</sup> Tomáš Polívka,<sup>‡</sup> Luca Dall’Osto,<sup>§</sup> Roberto Bassi,<sup>§</sup> and Harry A. Frank\*,<sup>†</sup>

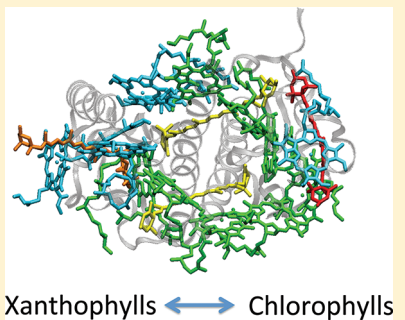
<sup>†</sup>Department of Chemistry, University of Connecticut, U-3060, 55 North Eagleville Road, Storrs, Connecticut 06269-3060, United States

<sup>‡</sup>Institute of Physical Biology, University of South Bohemia, Nove Hrady, Czech Republic

<sup>§</sup>Dipartimento di Biotecnologie, Università di Verona, Strada Le Grazie 15, I-37134 Verona, Italy

## S Supporting Information

**ABSTRACT:** The spectroscopic properties and energy transfer dynamics of the protein-bound chlorophylls and xanthophylls in monomeric, major LHCII complexes, and minor Lhcb complexes from genetically altered *Arabidopsis thaliana* plants have been investigated using both steady-state and time-resolved absorption and fluorescence spectroscopic methods. The pigment–protein complexes that were studied contain Chl *a*, Chl *b*, and variable amounts of the xanthophylls, zeaxanthin (Z), violaxanthin (V), neoxanthin (N), and lutein (L). The complexes were derived from mutants of plants denoted *npq1* (NVL), *npq2lut2* (Z), *aba4npq1lut2* (V), *aba4npq1* (VL), *npq1lut2* (NV), and *npq2* (LZ). The data reveal specific singlet energy transfer routes and excited state spectra and dynamics that depend on the xanthophyll present in the complex.



## INTRODUCTION

Green plants harvest solar energy using various pigment–protein complexes imbedded in the thylakoid membrane of chloroplasts.<sup>1,2</sup> A number of these complexes bound on the periphery of the Photosystem II (PSII) reaction center core may also be involved in the regulation of excited state energy flow in the photosynthetic apparatus and in the dissipation of light energy absorbed by plants in excess of that needed for photosynthesis.<sup>3</sup>

The major and most abundant pigment–protein complex in green plants is LHCII which exists in nature as a trimer of protein subunits arbitrarily assembled from three gene products denoted Lhcb1, Lhcb2, and Lhcb3.<sup>4,5</sup> The structure of the LHCII complex has been determined by X-ray crystallography by Liu et al.<sup>6</sup> to a resolution of 2.72 Å (Figure 1) in a preparation obtained from spinach and by Standfuss et al.<sup>7</sup> to 2.5 Å resolution in the pigment–protein complex prepared from peas. In both cases, the LHCII was reported to bind eight chlorophyll (Chl) *a* molecules, six Chl *b* molecules, and four xanthophylls per monomeric unit. On the stromal side of the membrane, two Chl *a* molecules per monomer form a tight inner six-membered ring of Chls that is highly suggestive of a role in transferring energy from one monomeric unit to the next. The remaining Chl *a* molecules on the stromal side of the membrane are arranged in groups of three per monomer protein unit and form an outer ring of pigments, alternating with clusters of three Chl *b* molecules. The remaining Chl *a* molecules are found on the luminal side of the protein at larger

distances from each other than those on the stromal side. Five Chl *b* molecules are found near one of the two protein interfaces joining neighboring monomeric units. One Chl *b* molecule resides at the other interface. Two all-trans-luteins (Lut) are located in each monomeric unit in the central region of the structure in sites denoted L1 and L2. Neoxanthin (Neo) was found to have a 9'-cis isomeric configuration<sup>8</sup> and to be bound in the Chl *b*-rich region of the protein in a site referred to as N1, thought to be highly specific for that xanthophyll.<sup>9,10</sup> A fourth xanthophyll binding site denoted V1 was located at the interface between monomeric protein units and was proposed to accommodate the binding of the carotenoids, violaxanthin (Vio), antheraxanthin (Anth), and zeaxanthin (Zea), known to be interconverted enzymatically in the xanthophyll cycle of higher plants.<sup>11</sup> The interconversion of these xanthophylls via this cycle has been correlated with excess energy dissipation.<sup>3,12</sup>

Less abundant than LHCII in green plants but also located on the periphery of the PSII core are the so-called minor, pigment-binding proteins, CP24 (Lhcb6), CP26 (Lhcb5), and CP29 (Lhcb4). In this work, the collection of Lhcb1, Lhcb2, and Lhcb3 proteins will be referred to as the major LHCII complex which can be isolated as monomers or trimers, and the combination of Lhcb4, Lhcb5, and Lhcb6 proteins will be referred to as the minor Lhcb monomer complexes. Each of the

Received: October 19, 2011

Revised: February 22, 2012

Published: February 28, 2012

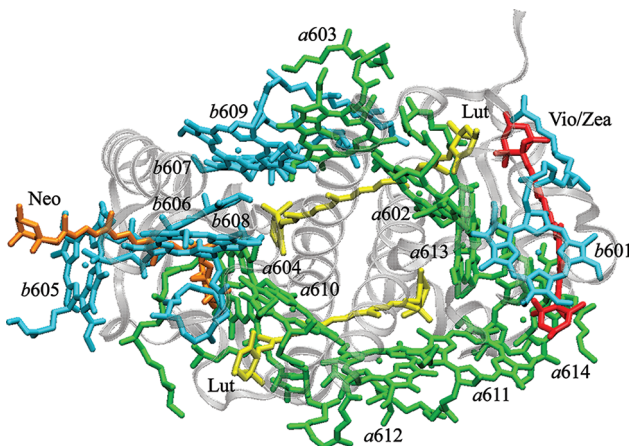


**Figure 1.** Structure and pigment composition in a monomer subunit of the major trimeric LHCII antenna protein of PSII. Green, Chl *a*; Blue, Chl *b*; orange, Neo in site N1; yellow, Lut occupying two binding sites denoted L1 and L2; and red, the xanthophyll cycle pigment binding site. The figure and notation were adapted from Liu et al.<sup>6</sup> and constructed using the coordinate set 1RWT deposited in the Brookhaven Protein Data Bank.

minor complexes exists in roughly a 1:1 stoichiometric ratio with the PSII reaction center.<sup>13–16</sup> These proteins have been reported to be enriched in xanthophyll cycle carotenoids compared to LHCII, suggesting that excess energy dissipation may be closely associated with them.<sup>13,17</sup> Recently, a 3-D structure of the CP29 complex has been reported by X-ray diffraction to 2.80 Å resolution.<sup>18</sup> This and the X-ray structures of the LHCII complex<sup>6,7</sup> are major breakthroughs helping to visualize which pigment molecules are involved in regulating the flow of energy and which are acting as energy quenching sites. Yet, despite extensive biochemical, structural, and spectroscopic investigations of the LHCII and LhcB pigment–protein complexes,<sup>19–25</sup> the pathways by which energy is transferred to and from xanthophylls and Chls within the complexes and between protein units are still not entirely clear. Moreover, the specific protein-bound pigments involved in quenching excess excited state energy of Chl have not yet been identified, nor has consensus been reached regarding the molecular mechanism of nonradiative energy dissipation. The electronic structures of the pigments and pigment–pigment and pigment–protein interactions are complicated, and structural changes can modulate the rates and efficiencies of the processes of energy transfer and energy dissipation that take place after photoexcitation.

Xanthophylls function as antenna pigments by absorbing light in a region of the visible spectrum where Chl is not an efficient absorber and then transferring the energy to Chl. Light absorption by xanthophylls occurs via a transition from the ground state,  $S_0$ , to the second excited singlet state,  $S_2$ . The  $S_0 \rightarrow S_2$  transition is strongly allowed. The transition from  $S_0$  to the lowest-lying excited singlet state,  $S_1$ , is forbidden by symmetry selection rules.<sup>26,27</sup> The excited xanthophyll may either transfer energy from the  $S_2$  state directly to Chl *a* or *b*, or it may undergo internal conversion to the  $S_1$  state. Both of these processes occur on the order of a few hundred femtoseconds. After being populated from the  $S_2$  state,  $S_1$  may transfer energy to the Chls or relax back to the ground state. Chls act as energy acceptors using their low-lying  $S_1$  and  $S_2$  excited states which correspond to allowed transitions denoted  $Q_Y$  and  $Q_X$ , respectively. The extent to which the

excited state energy is partitioned among these various states and molecules, and the rates and efficiencies of the various pathways, can be measured using ultrafast time-resolved spectroscopic methods.<sup>19–21,25,28–36</sup>

The mechanism by which excess excited state energy of Chl *a* is quenched in green plants has been proposed to involve either the major LHCII protein complex or the minor LhcB (CP24, CP26, and CP29) systems, or both. At least four models exist: in one model quenching is proposed to result from aggregation of the major trimeric LHCII complex which produces a conformational change that opens an energy transfer pathway to the  $S_1$  state of Lut which then deactivates the excess Chl excited state energy.<sup>37,38</sup> In another model, energy from bulk Chls is trapped by a Chl/Zea heterodimer which undergoes charge transfer to form a Zea radical cation/Chl radical anion pair followed by subsequent charge recombination as the means of deactivating excess Chl *a* excited states.<sup>39,40</sup> A third model proposes that Zea/Chl exciton coupling provides a pathway for deactivation of excess excited Chl via the rapidly decaying  $S_1$  state of the xanthophyll.<sup>41–43</sup> A fourth model suggests that oligomerization of LHCII trimers leads to the formation of Chl/Chl exciton pairs which undergo charge transfer as the pathway for Chl excited state deactivation.<sup>44–46</sup>

There are major obstacles to determining which of these mechanisms is active. These include the ultrafast nature of the photoprocesses which require sophisticated spectroscopic methodologies to probe the excited state spectra and dynamics of the pigments, overlapping absorption spectral lineshapes which make it difficult to excite selectively and monitor the behavior of one protein-bound pigment at a time, the difficulty in preparing ample quantities of ultrapure protein samples for the experiments, and the inherent problem of relating the experimental data taken on purified proteins to the quenching process *in vivo*.

In this work, we present the results of a steady-state and ultrafast time-resolved spectroscopic investigation of 12 different monomeric LHCII and LhcB pigment–protein complexes isolated from *Arabidopsis thaliana* plants that have undergone mutagenesis affecting the xanthophyll biosynthetic pathway. The mutations lead to the accumulation of specific xanthophylls or combinations of xanthophylls in the plants. The *Arabidopsis thaliana* mutants are *npq1*, which inhibits the violaxanthin de-epoxidase enzyme needed to convert Vio to Zea, and therefore accumulates only Neo, Vio, and Lut;<sup>3</sup> *npq2*, which inhibits the zeaxanthin epoxidase enzyme needed to convert Zea back to Vio, and therefore accumulates only Lut and Zea;<sup>3</sup> *npq2lut2*, the *lut2* part of which disrupts the epsilon-ring cyclization reaction that is required to form Lut.<sup>47</sup> Therefore, this double mutant accumulates only Zea; *npq1lut2*, which is incapable of forming Zea or Lut. Hence, it accumulates only Vio and Neo; *aba4npq1*, which in addition to inhibiting the violaxanthin de-epoxidase enzyme that forms Zea via *npq1* uses the *aba4* mutation to inhibit Neo synthesis.<sup>47</sup> Thus, this double mutant accumulates only Vio and Lut; *aba4npq1lut2*, which adds the *lut2* mutation to the *aba4npq1* mutant resulting in the accumulation of only Vio in the plant. A list of the LHCII and LhcB complexes prepared from mutant *Arabidopsis thaliana* plants and used in the current study is given in Table 1. Steady-state and time-resolved absorption and fluorescence spectroscopic experiments were carried out on all the samples. Analyses of the ground and excited state spectra and dynamics revealed specific spectroscopic observables associated with energy and electron transfer reactions in the pigment–protein

**Table 1. Pigment–Protein Complexes from *Arabidopsis thaliana* Used in the Present Work<sup>a</sup>**

LHCII complexes	Lhcb complexes
LHCII (NVL) <i>npq1</i>	Lhcb (NVL) <i>npq1</i>
LHCII (Z) <i>npq2lut2</i>	Lhcb (Z) <i>npq2lut2</i>
LHCII (V) <i>aba4npq1lut2</i>	Lhcb (V) <i>aba4npq1lut2</i>
LHCII (VL) <i>aba4npq1</i>	Lhcb (VL) <i>aba4npq1</i>
LHCII (NV) <i>npq1lut2</i>	Lhcb (NV) <i>npq1lut2</i>
LHCII (LZ) <i>npq2</i>	Lhcb (LZ) <i>npq2</i>

<sup>a</sup>All of the proteins were monomeric. The letters in capitals refer to the xanthophyll composition: N, neoxanthin; V, violaxanthin; L, lutein; Z, zeaxanthin. The code in italics refers to the type of mutation that resulted in the accumulation of specific xanthophylls in the plants.

complexes. The experiments have examined the roles of individual xanthophylls or specific combinations of xanthophylls in these photoprocesses and have addressed the photochemical behavior of the isolated pigment–protein complexes containing these molecules.

## MATERIALS AND METHODS

**Plant Material and Growth Conditions.** *Arabidopsis thaliana* individual T-DNA insertion mutants (*Columbia* ecotype) were obtained as described previously.<sup>48–50</sup> Double and triple mutants were obtained by crossing single mutant plants and selecting progeny by pigment analysis after high-light treatment. Plants were grown on compost in a growth chamber for 6 weeks under controlled conditions (100 μmol photons m<sup>-2</sup> s<sup>-1</sup>, 21 °C, 80% humidity, and 8 h of daylight).

**Preparation of Complexes.** Unstacked thylakoids were isolated from leaves as previously described.<sup>51</sup> Membranes corresponding to 500 μg of Chl were washed with 5 mM EDTA and then solubilized in 1 mL of 0.6% α-dodecylmalto-side (α-DM) and 10 mM HEPES, pH 7.5. Solubilized samples were then fractionated by ultracentrifugation at 4 °C for 22 h at 280 000g in a 0.1–1 M sucrose gradient containing 0.06% α-DM and 10 mM HEPES, pH 7.5. Monomeric Lhcb proteins migrated as the second band from the top of the gradient. This band was collected, concentrated to 1 mg Chl/mL using a centrifugal filter (Vivaspin 500, Sartorius, Ge), and further fractionated by flatbed isoelectrofocusing at 4 °C as previously described.<sup>52</sup> Green bands were harvested and loaded into a second 0.1–1 M sucrose gradient which was spun for 26 h at 280 000g at 4 °C to eliminate unbound pigments and carrier amphophytes which resided in the top band. The monomeric Lhcb proteins (second band from the top) were collected, frozen in aliquots in liquid nitrogen, and stored at –80 °C until ready for use in the spectroscopic experiments.

**Pigment Analysis.** Pigments were extracted from the isolated complexes with buffered 85% acetone (v/v) and fractionated and quantified by high-performance liquid chromatography (HPLC) as described previously.<sup>53</sup> The uncertainties in the pigment composition were determined by analyzing multiple replicate samples and by integrating the areas of the observed HPLC peaks calibrated using pure xanthophyll standards.

**Steady-State Spectroscopic Methods.** Steady-state absorption spectroscopy was carried out at room temperature using a Varian Cary 50 UV–visible spectrophotometer. Steady-state fluorescence and fluorescence excitation spectra were recorded using a Jobin-Yvon Horiba Fluorolog-3 model FL3-22 equipped with double monochromators having 1200 grooves/

mm gratings, a Hamamatsu R928P PMT emission detector, and a 450 W ozone-free Osram XBO xenon arc lamp. The fluorimeter was set to right-angle emission collection with respect to the excitation beam. The samples were held in a quartz cuvette having a path length of 4 mm for emission spectra and 1 cm for excitation spectra. The emission spectra were recorded using 650 nm excitation, with a bandpass corresponding to 2 nm for the excitation monochromator and 1 nm for the emission monochromator. To correct for the wavelength dependence of the optical components and the fluctuations in lamp intensity, the emission signal was divided by a calibrated lamp profile generated by a reference photodiode.

**Time-Resolved Fluorescence.** Time-resolved fluorescence spectroscopy was performed using a time-correlated single-photon counting module installed on the Jobin-Yvon Horiba Fluorolog-3. A pulsed NanoLED-670L diode light source generating 665 nm light with a pulse duration of <200 ps was used for excitation. The repetition rate was 1 MHz. The time response profiles were recorded at 680 nm and were fitted using a sum of exponentials function.

**Femtosecond Time-Resolved Transient Absorption.** Femtosecond transient pump–probe absorption experiments were carried out using a Helios transient absorption spectrometer (Ultrafast Systems, LCC), coupled to a femtosecond laser system previously described.<sup>54</sup> The system is based on a Spitfire-50 fs, Ti:sapphire amplifier with pulse stretcher and compressor (Spectra-Physics) pumped at a 1 kHz repetition rate by an Evolution 15, Q-switched Nd:YLF laser (Coherent) and seeded by pulses from a Tsunami, mode-locked Ti:sapphire oscillator (Spectra-Physics) pumped by a Millenia VsJ, diode-pumped Nd:YVO<sub>4</sub> CW visible laser (Spectra Physics). Output pulses having a wavelength of 800 nm, an energy of 600 μJ/pulse, a duration of ~50 fs, and a 1 kHz repetition rate were split into two beams by a beamsplitter. Ninety percent of the signal was sent to an OPA-800C optical parametric amplifier (Spectra-Physics) to generate the pump beam. The remaining 10% was used to derive probe pulses. A white light continuum probe of 450–800 nm in the visible region and 850–1450 nm in the near-infrared (NIR) was generated by a 3 mm Sapphire plate. A charge-coupled detector S2000 with a 2048 pixel array from Ocean Optics was used as a detector in the visible range. In the NIR, a 512 pixel array SU-LDV high-resolution InGaAs Digital Line Camera from Sensors Unlimited was used. The pump and probe beams were overlapped at the sample at the magic-angle (54.7°) polarization. The signals were averaged over 5 s. The samples were excited by the pump beam tuned to either 490 nm which excited both the S<sub>2</sub> state of the xanthophylls and the Soret band of Chl *b* or 676 nm which excited the Q<sub>y</sub> band of Chl *a*. The energy of the pump beam was 1 μJ/pulse in a spot size of 1 mm diameter. This corresponds to an intensity of 3.0 to 5.4 × 10<sup>14</sup> photons/cm<sup>2</sup> pulse. The optical densities (ODs) of the samples were 0.4–0.7 in a 2 mm cuvette at the excitation wavelength. The samples were mixed continuously using a magnetic microstirrer to prevent photodegradation. The integrity of the samples was checked by taking a steady-state absorption spectrum before and after every experiment.

## RESULTS

**Biochemical Characterization of the Pigment–Protein Complexes.** We have isolated LHCII and Lhcb pigment–protein complexes from *Arabidopsis thaliana* mutant plants

having altered xanthophyll compositions (Table 1). LHCII is believed to be present in thylakoids mainly as a trimer, although it can be easily dissociated into monomeric components. In the absence of Lut, LHCII is found in its monomeric form only. To avoid heterogeneity in the aggregation state of the complexes, we purified the monomeric fraction of LHCII and disregarded trimers. The minor, monomeric antenna complexes, CP24 (Lhc6), CP26 (Lhc5), and CP29 (Lhc4), comigrate with the monomers of LHCII in band 2 after ultracentrifugation. These two classes of antenna complexes were separated from each other by flat-bed isoelectrofocusing (IEF). Fractions with  $pI < 3.9$  contained the major LHCII (Lhc1–3) complex, whereas fractions with  $pI > 4.1$  contained the minor Lhc complexes (Lhc4–6). Fractions eluted from the IEF slurry were subjected to a second step of sucrose gradient ultracentrifugation to separate the unbound pigments and carrier ampholytes and to make sure that all complexes were in a monomeric form. These green fractions containing either monomeric LHCII or a mixture of the minor Lhc complexes were collected and analyzed for pigment and protein composition. The results of an SDS-PAGE analysis of the Lhc and LHCII preparations are shown in the Supporting Information (Figure S1 and Table S1). The pigment content of LHCII from *npq1* plants (Table 2) includes Chl *a*, Chl *b*, and the three xanthophylls, Lut, Neo, and Vio, in a relative ratio of 8 (Chl *a*):6 (Chl *b*):2 (Lut):0.7 (Neo):0.3 (Vio), implying the binding of three xanthophylls per polypeptide.

In comparing these results with those from trimeric LHCII from spinach, it was observed that while the Chl complement was the same (8 Chl *a* and 6 Chl *b* molecules, Chl *a/b* ratio of 1.33) the xanthophyll content was lower (Chl/Car ratio found here is 4.77 vs the value of 3.5 found by Liu et al.<sup>6</sup>), and LHCII (NVL) is particularly low in Vio (Table 2). This is consistent with previous results showing that the IEF procedure which isolates monomers removes the xanthophyll ligand from the labile site V1 in LHCII.<sup>5</sup> Thus, the xanthophylls in the present LHCII complexes are bound to the sites L1, L2, and N1, while the V1 site is empty. The present data are also consistent with the occupancy of site N1 in LHCII (NVL) by both Neo and Vio (Neo/Vio ratio 0.75:0.30), while the crystallographic data reveal the presence of Neo only. Although this might be a species-specific difference, it should be noted that Neo and Vio have the same structure on the part of the molecule bound to the complex,<sup>6</sup> whereas in the absence of Neo, e.g., for LHCII (V), the site can be occupied by Vio.<sup>55</sup> All LHCII samples bind ~3 (2.85–3.08) xanthophylls per 14 Chls (Table 2), the only exception being LHCII (Z) from *npq2lut2* which binds 2.42 xanthophyll molecules. When either Vio (mutant *aba4npq1-lut2*) or Zea (mutant *npq2lut2*) is present as the sole xanthophyll, the corresponding antenna complexes (LHCII (V) and LHCII (Z), respectively) showed a significantly lower Chl *a/b* ratio (1.06 in LHCII (V), 1.18 in LHCII (Z)) and a higher Chl/Car ratio (4.91 in LHCII (V), 5.79 in LHCII (Z)). On the basis of biochemical analysis, it cannot be determined if there was a substitution of Chl *a* with Chl *b* in some binding site or if Chl *b* was preferentially lost. The first hypothesis is favored since Lhc proteins have been reported to have sites with mixed occupancy,<sup>56,57</sup> and different Chl *a/b* ratios can be obtained depending on folding conditions in vitro<sup>58</sup> and in vivo.<sup>49,58</sup> Assuming that 14 Chls per polypeptide are present in both complexes, a xanthophyll composition of 2.85 molecules per polypeptide is obtained in LHCII (V), and 2.42 is found for LHCII (Z). In both of these LHCII samples, Neo was absent;

Table 2. Pigment Composition of the LHCII and Lhc Complexes<sup>a</sup>

genotype	sample	Chl <i>a/b</i>	Chls/Cars	mol Chls/14 mol Chls				
				Neo	Vio	Anth	Lut	Zea
monomeric Lhc	Lhc (NVL)	1.89 ± 0.02	4.77 ± 0.02	0.72 ± 0.01	0.64 ± 0.01	-	1.57 ± 0.01	-
	Lhc (V)	1.36 ± 0.01	4.99 ± 0.02	-	2.39 ± 0.01	0.24 ± 0.01	-	0.16 ± 0.01
	Lhc (Z)	1.97 ± 0.02	5.21 ± 0.01	-	-	-	1.63 ± 0.01	2.69 ± 0.01
	Lhc (VL)	2.10 ± 0.02	4.51 ± 0.01	-	1.47 ± 0.01	-	-	3.10 ± 0.01
	Lhc (INV)	1.77 ± 0.02	4.48 ± 0.01	0.78 ± 0.01	1.74 ± 0.01	0.47 ± 0.01	-	0.14 ± 0.01
	Lhc (LZ)	1.90 ± 0.01	5.02 ± 0.01	-	-	1.27 ± 0.01	1.52 ± 0.01	3.12 ± 0.01
monomeric LHCII	LHCII (NVL)	1.30 ± 0.02	4.77 ± 0.03	0.75 ± 0.01	0.30 ± 0.01	-	1.89 ± 0.01	-
	LHCII (V)	1.06 ± 0.01	4.91 ± 0.01	-	2.46 ± 0.01	0.28 ± 0.01	-	0.11 ± 0.01
	LHCII (Z)	1.18 ± 0.02	5.79 ± 0.02	-	-	-	-	2.42 ± 0.01
	LHCII (VL)	1.28 ± 0.01	4.54 ± 0.07	-	0.93 ± 0.01	-	2.15 ± 0.02	-
	LHCII (NV)	1.10 ± 0.01	4.70 ± 0.01	0.92 ± 0.02	1.61 ± 0.02	0.35 ± 0.01	-	0.11 ± 0.01
	LHCII (LZ)	1.29 ± 0.01	4.97 ± 0.04	-	-	-	1.79 ± 0.01	1.02 ± 0.01

<sup>a</sup>The uncertainties in the pigment composition were determined from the reproducibility of the HPLC results as described in the text.

however more than two xanthophyll molecules were bound to these LHCII. Because Lut cannot bind to site N1,<sup>50,59</sup> this implies that the N1 site can be occupied by Vio or Zea in samples lacking Neo. Also, because *aba4npq1lut2* plants accumulate a small amount of Anth and Zea even in their dark-adapted state due to accumulation of metabolic intermediates, LHCII (V) purified from these plants retain a small amount of tightly bound Zea plus Anth, viz., a total of ~0.4 mol of xanthophylls per mole of polypeptide.

Monomeric LHCII isolated from the other genotypes bind two different xanthophylls: Vio and Lut (in *aba4npq1*), Neo and Vio (in *npq1lut2*), and Lut and Zea (in *npq2*). Assuming that 14 Chl per polypeptide are present in both complexes, a xanthophyll content of 2.82–3.08 molecules per polypeptide is obtained in all the complexes. In all cases, Chl *a/b* ratios are reduced with respect to LHCII from *npq1* (LHCII (NVL)) as an effect of altered xanthophyll composition. The reduction is small for the LHCII (LV) and LHCII (LZ) samples (compare the ratio of 1.30 for LHCII (NVL) to the ratios of 1.28 and 1.29 for these complexes, respectively), while it is more pronounced for LHCII (NV) which has a ratio of 1.10 (Table 2).

In the LHCII (VL) complex, the Lut/Vio ratio was found to be ~2, suggesting that Vio may bind to the site N1, as previously reported for *Arabidopsis thaliana*.<sup>55</sup> LHCII (NV) showed a Vio/Neo ratio of 1.75 and a (Vio+Anth+Zea)/Neo ratio of 2.2. In this complex, the lack of Lut is compensated by binding Vio and, to a lesser extent, Anth and Zea in sites L1 and L2. In LHCII (LZ), the Lut/Zea ratio is 1.75, while the complex binds 2.82 xanthophylls per polypeptide, confirming that Zea can bind to the N1 site even though the affinity of Zea to the N1 site is lower than for Neo or Vio.

Samples denoted here as Lhcbs are a mixture of CP24, CP26, and CP29 proteins, each having different Chl and xanthophyll compositions.<sup>18,51,58</sup> Thus, the pigment binding site occupancy of each subunit was not individually determined in the present work, and the effect of mutation in the xanthophyll biosynthesis pathway on the pigment composition of the Lhcbs can only be considered as an average effect on the three subunits.

Lhcbs (NVL) complexes from *npq1* showed a higher Chl *a/b* ratio than the corresponding LHCII (1.89 vs the value of 1.30 in LHCII (NVL)). While the Chl/Car ratio of 4.77 is in agreement with a previous report,<sup>13</sup> Lhcbs (NVL) was enriched in xanthophyll cycle carotenoids with respect to LHCII. (The Vio/Lut ratio was found to be 0.40 vs 0.15 for LHCII.) Altering the xanthophyll content in the minor Lhcbs results in changes in both the Chl *a/b* and Chl/Car ratios: when Vio is the only xanthophyll, the corresponding Lhcbs showed a lower Chl *a/b* ratio (1.36 in Lhcbs (V) vs 1.89 in Lhcbs (NVL)) and a higher Chl/Car ratio (4.99 in Lhcbs (V) vs 4.77 in Lhcbs (NVL)); in these complexes, the lack of both Lut and Neo is mostly compensated by binding of Vio and of stoichiometric amounts of Anth and Zea (a total of ~0.2 mol of xanthophylls per mole of Chl). In Lhcbs (Z), higher Chl *a/b* and Chl/Car ratios (1.97 and 5.21, respectively) were found with respect to that in Lhcbs (NVL) which were 1.89 and 4.77.

Lhcbs isolated from the (NV), (VL), and (LZ) genotypes bind two xanthophyll species each. In comparing these samples with respect to the control Lhcbs (NVL) sample, the major differences include: (i) an increase of Chl *a/b* ratio whenever Neo is missing (2.10 in Lhcbs (VL), 1.90 in Lhcbs (LZ) vs 1.89 in Lhcbs (NVL)); (ii) a higher Chl/Car ratio in Lhcbs (LZ) (5.02 vs 4.77 in Lhcbs (NVL)), while this value drops to ~4.50

when either Neo or Lut are missing (Table 2). As noted above for LHCII, the lack of either Neo or Lut in Lhcbs complexes is mostly compensated by binding Vio (in Lhcbs (VL) and Lhcbs (NV)) or Zea (in Lhcbs (LZ)).

### Steady-State Absorption and Fluorescence Spectra.

Figure 2 shows the steady-state absorption spectra of the Lhcbs

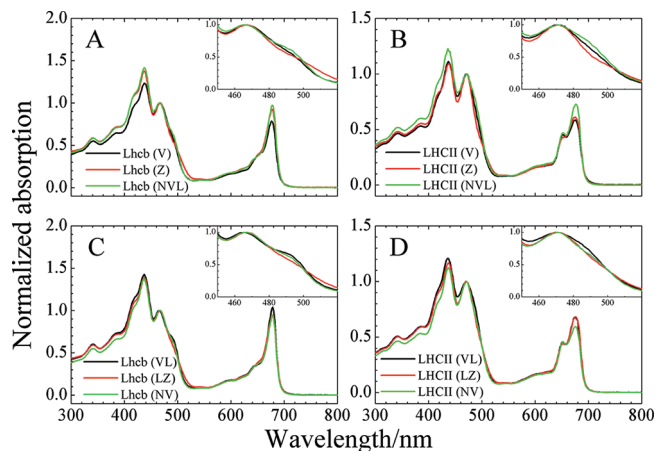


**Figure 2.** Steady-state absorption spectra of the (A, C) minor (Lhcbs) and (B, D) major (LHCII) pigment–protein complexes from *Arabidopsis thaliana*. The letters N, V, L, and Z refer to the xanthophyll composition: N, neoxanthin; V, violaxanthin; L, lutein; Z, zeaxanthin. The insets provide an expanded view of the xanthophyll absorption bands.

and LHCII complexes. The primary features include for Chl *a* a Soret band at 440 nm and a Q<sub>y</sub> band at 676 nm, for Chl *b* a Soret band at 470 nm and a Q<sub>y</sub> band at 650 nm, and xanthophyll absorption bands between 480 and 510 nm. The insets in Figure 2 show an expanded view in the region of xanthophyll absorption, emphasizing the spectral changes due to the different pigment compositions of the complexes. Note for example that the complexes containing Zea have xanthophyll absorption bands that extend to longer wavelength than those without Zea. (See, e.g., the red trace in Figure 2A.) This is due primarily to the broader spectral line shape of Zea compared to Vio.

Steady-state fluorescence spectra of the Lhcbs and LHCII complexes are shown in Figure 3. The samples were excited at 650 nm corresponding to the maximum of the Chl *b* Q<sub>y</sub> absorption. All samples were adjusted to an optical density corresponding to 0.037 at the excitation wavelength in a 4 mm path length cuvette to compare directly the relative fluorescence yields of the samples. The fluorescence spectra of the Lhcbs complexes (Figure 3A) exhibit a maximum in their emission spectra at  $680 \pm 1$  nm. The fluorescence spectra of the LHCII complexes (Figure 3B) are slightly red-shifted relative to the Lhcbs complexes and have a maximum at  $682 \pm 1$  nm.

The steady-state fluorescence spectra of the complexes shown in Figure 3 reveal that differences in the xanthophyll pigment composition can influence the yield of Chl *a* emission. For both the Lhcbs and LHCII complexes, the fluorescence intensity is lowest when Zea is the sole xanthophyll present. This is particularly noticeable when one compares the spectra of the complexes containing only Vio (Lhcbs (V) and LHCII (V)) to those containing only Zea (Lhcbs (Z) and LHCII (Z), Figure 3C). However, it is also observed that the fluorescence

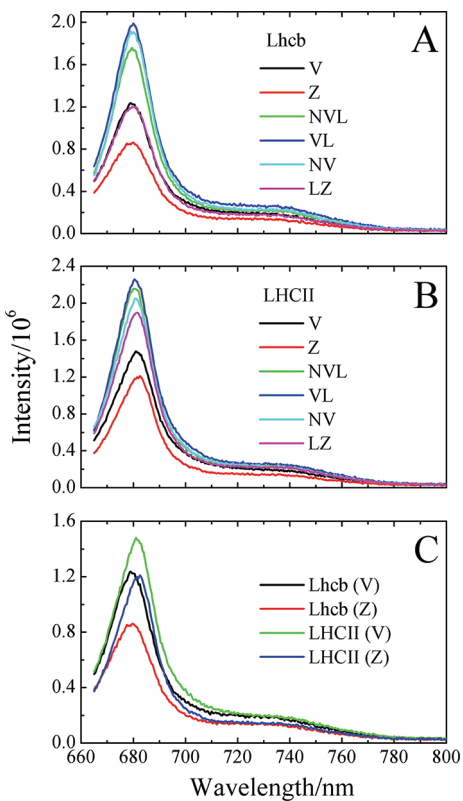


**Figure 3.** Steady-state emission spectra of (A) LhcB and (B) LHCII containing V, L, NVL, VL, NV, and LZ after excitation at 650 nm. Emission spectra of LhcB and LHCII containing only V and only Z are compared in (C). The samples were adjusted to the same OD at the excitation wavelength.

intensity of the LhcB (LZ) complex has lower fluorescence intensity relative to the LhcB (VL) (Figure 3A). A similar situation exists regarding the fluorescence intensity of the LHCII (LZ) complex which has lower fluorescence intensity compared to the LHCII (VL) complex (Figure 3B). Thus, the presence of Lut in the complex along with Vio or Zea does not change the fact that the samples containing Zea exhibit a lower amount of Chl *a* fluorescence compared to those with Vio. It is also observed that the complexes containing exclusively Vio or Zea have lower fluorescence intensities compared with complexes containing Vio or Zea along with Lut or Neo. This is seen, for example, by comparing the fluorescence intensity of the LhcB (V) (black line in Figure 3A) with that from LhcB (VL) (blue line in Figure 3A) or by comparing the fluorescence intensity of the LhcB (Z) (red line in Figure 3A) with that from LhcB (LZ) (purple line in Figure 3A). Additionally, the emission bands of all the LHCII mutants were uniformly more intense than those of their LhcB counterparts; e.g., LHCII (V) has a higher fluorescence intensity than LhcB (V) (Figure 3C).

**Fluorescence Excitation Spectroscopy.** Figure 4 shows the fluorescence excitation spectra (red lines) of the LhcB and LHCII complexes overlaid with the 1-T spectra (black lines), where *T* is transmittance. There are two observations worthy of note. First, for the LhcB (V), LhcB (Z), LHCII (V), and LHCII (Z) complexes (top four panels in Figure 4), the excitation spectra do not match well with the 1-T spectra in the region of the Chl *b* Q<sub>y</sub> band absorption. This indicates that in these complexes energy transfer from Chl *b* to Chl *a* is not 100%

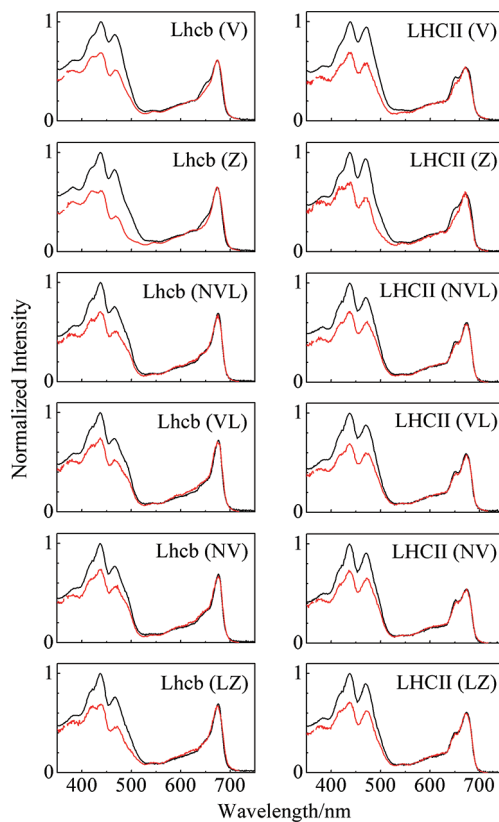


**Figure 4.** Overlay of fluorescence excitation (red lines) and 1-T spectra, where *T* is transmittance (black lines) recorded for the LhcB and LHCII complexes. The excitation spectra were monitored at 730 nm. The intensities of excitation and 1-T spectra were normalized at the maximum of the Chl *a* Q<sub>y</sub> band.

efficient. For all the other complexes, the agreement between the excitation and 1-T spectra in this region is very good, indicating a high efficiency of energy transfer from Chl *b* to Chl *a*. Second, in the region of the Chl *b* Soret band at 470 nm and the xanthophyll absorption between 450 and 525 nm, the agreement between the excitation and 1-T varies depending on the complex and the xanthophyll bound. Overall, only about 50% of the photon energy absorbed in this region is transferred to Chl *a* which is consistent with previous findings that the efficiency of energy transfer from bound xanthophylls to Chl *a* varies from ~50 to 80% in the LHCII complex.<sup>22</sup> However, the complexes containing Vio show much better agreement between the excitation and 1-T spectra than the complexes containing Zea. For example, a comparison of the spectral overlays of LhcB (V) and LhcB (Z) (top two panels in the left-hand column of Figure 4) or of LHCII (V) and LHCII (Z) (top two panels in the right-hand column of Figure 4) reveals that on the long wavelength side of the xanthophyll absorption bands near 500 nm there is much better agreement between the excitation and 1-T spectra for the complexes containing Vio compared to those containing Zea. This indicates that Vio transfers excited state energy much more efficiently to Chl *a* than Zea. Spectral overlays of the other complexes lead to the same conclusion; i.e., a comparison of the excitation and 1-T spectra of LhcB (VL) with those of LhcB (LZ) or LHCII (VL) with LHCII (LZ) indicates that the complexes containing Vio are more efficient at transferring energy to Chl *a* than those containing Zea.

**Time-Resolved Fluorescence.** The effect that different xanthophyll compositions in the light-harvesting complexes have on the kinetic components associated with fluorescence decay was investigated using time-correlated single-photon counting spectroscopy. The complexes were excited at 665 nm, and the Chl *a* fluorescence was detected at 680 nm. The kinetics derived from a fit to a sum of exponentials function are given in Table 3. For all the complexes, three kinetic

**Table 3. Lifetimes and Amplitudes (Expressed As a Percent of the Total) of the Time-Resolved Fluorescence Components Detected at 680 nm Using 665 nm Excitation<sup>a</sup>**

	$\tau_1/\text{ns}$	$A_1/\%$	$\tau_2/\text{ns}$	$A_2/\%$	$\tau_3/\text{ns}$	$A_3/\%$	$\tau_{\text{ave}}/\text{ns}$
Lhcb (V)	0.9	17	3.0	57	6.0	26	2.4
Lhcb (Z)	0.6	38	2.0	35	5.9	27	1.2
Lhcb (NVL)	0.5	15	3.0	58	5.6	27	1.8
Lhcb (NV)	0.7	16	3.2	69	5.9	15	2.1
Lhcb (VL)	0.8	18	3.5	65	6.1	17	2.3
Lhcb (LZ)	0.6	32	2.1	44	5.7	25	1.3
LHCII (V)	1.3	16	3.0	67	6.0	17	2.7
LHCII (Z)	1.0	33	2.3	57	6.1	10	1.7
LHCII (NVL)	0.8	15	3.5	75	6.5	9	2.4
LHCII (NV)	0.7	9	2.9	78	5.8	13	2.4
LHCII (VL)	0.8	12	3.2	67	5.5	20	2.5
LHCII (LZ)	1.0	16	3.1	67	5.8	17	2.5

<sup>a</sup>The average lifetimes,  $\tau_{\text{ave}}$ , were calculated from a sum of the amplitude-weighted rate constants.

components were sufficient to fit the transient fluorescence data. The lifetimes of these components were within three reasonably narrow time ranges for all the complexes, but their amplitudes were noticeably different depending on which xanthophyll was present.

The fastest fluorescence decay component was found to have a lifetime ranging from 0.5 to 1.3 ns. This component was most pronounced in the Zea-containing complexes, Lhcb (Z), Lhcb (LZ), and LHCII (Z), where it represented approximately one-third of the fluorescence decay amplitude. In the corresponding complexes containing Vio, Lhcb (V) and Lhcb (VL), and LHCII (V) and in all of the other complexes, this component contributed less than 20% of the amplitude to the overall fit. The next fastest component was found to have a lifetime ranging from 2.0 to 3.5 ns. This component dominates the fluorescence amplitude representing approximately two-thirds of the fluorescence decay amplitude in all cases except Lhcb (Z) and Lhcb (LZ) where it was determined to be 35% and 44%, respectively. Also, it is interesting to note that the lifetime of this component in both the Lhcb (V) and LHCII (V) complexes which contain only Vio was 3.0 ns, whereas for the Lhcb (Z) and LHCII (Z) complexes which contain only Zea, the lifetime was significantly shorter at 2.0 and 2.3 ns, respectively. The lifetime of this component was also shorter for Lhcb (LZ) (2.1 ns) compared to Lhcb (VL) (3.5 ns). The third component was found to have a lifetime between 5.5 and 6.5 ns and showed no obvious dependence of amplitude or lifetime on the xanthophyll composition. Because 6 ns is quite close to the fluorescence lifetime of free Chl *a* in solution, it is reasonable to ask whether this component might arise from disconnected Chl in the samples. We do not believe this is the case since the proteins were highly purified, and their stability was assayed by taking absorption spectra before and after every spectroscopic experiment. If the complexes were unstable,

evidence of this should appear in the Chl Q<sub>V</sub> bands because they are very sensitive to the local environment. More likely, due to structural changes resulting from binding the different xanthophylls, there may be Chls that are less coupled to other bound Chls in the protein, rendering their kinetic behavior analogous to free Chl.

### Femtosecond Time-Resolved Absorption Spectra.

Transient absorption spectra of the Lhcb complexes taken at various delay times after laser excitation are presented in Figure 5. Spectra in the visible region recorded upon excitation at 490 nm (left-hand column in Figure 5) show the immediate onset of bleaching of the xanthophyll absorption bands between 475 and 525 nm as well as bleaching of the Chl *a* and *b* Q<sub>V</sub> absorption bands at 685 nm and 652 nm, respectively. Subsequently, there is a buildup of characteristic carotenoid S<sub>1</sub> → S<sub>N</sub> transient absorption bands between 530 and 580 nm which persist for several picoseconds. The Chl *b* band bleaching decays in less than 5 ps, but the Chl *a* band bleaching remains for several nanoseconds. NIR spectra recorded after 490 nm excitation (second column in Figure 5) show a short-lived xanthophyll S<sub>2</sub> → S<sub>N</sub> transition between 950 and 1200 nm peaking at ~1000 nm (black lines in Figure 5). For the samples containing Vio (Lhcb (V), Lhcb (NVL), Lhcb (NV), and Lhcb (VL)), this band is superimposed with another transition that appears at ~910 nm. The S<sub>2</sub> → S<sub>N</sub> transition decays in a few hundred femtoseconds, but the peak at ~910 nm remains. For the samples containing Zea, no ~910 nm peak is evident, but after a few hundred femtoseconds there remains a broader band with a maximum at ~990 nm. Also in this spectral region, weak bands associated with long-lived Chl *a* S<sub>1</sub> → S<sub>N</sub> and xanthophyll S<sub>1</sub> → S<sub>2</sub> excited state transitions between 1050 and 1200 nm are observed. Spectra taken in the visible wavelength region after excitation at 676 nm (third column in Figure 5) show primarily bleaching of the Q<sub>V</sub> band of Chl *a* at 681 nm but also have a weak positive signal in the spectral region between 480 and 560 nm which is particularly noticeable for the Lhcb (V) complex. For the samples containing Zea there is also a weak positive signal in this region, but it is much broader and red-shifted compared to that seen for the samples containing Vio. NIR spectra measured using 676 nm excitation (fourth column in Figure 5) show bands at 890 and 1080 nm that persist for tens of picoseconds and are common to all of the complexes. This indicates that they are not associated with xanthophylls but rather are due to Chl *a* excited state absorption. However, in the samples containing Zea, i.e., Lhcb (Z) and Lhcb (LZ), excited at 676 nm, there also appears a small signal at ~990 nm in the 50 ps traces (red lines) which may be assigned to a Zea<sup>•+</sup> radical cation.

Transient absorption spectra of the LHCII complexes taken in the visible and NIR regions at various delay times after laser excitation at either 490 or 676 nm are very similar to those observed for the Lhcb complexes and are presented in Figure S2 (Supporting Information). The main differences in these spectra are that no signals at ~990 nm attributable to the Zea<sup>•+</sup> radical cation are observed in any of the complexes including LHCII (Z) and LHCII (LZ).

## DISCUSSION

**Absorption Spectra.** To understand the contributions of each pigment to the steady-state spectra shown in Figure 2, fitting of the spectra in the wavelength region between 400 and 540 nm containing the Chl *a* and *b* Soret bands and the xanthophyll absorption features was carried out for the Lhcb

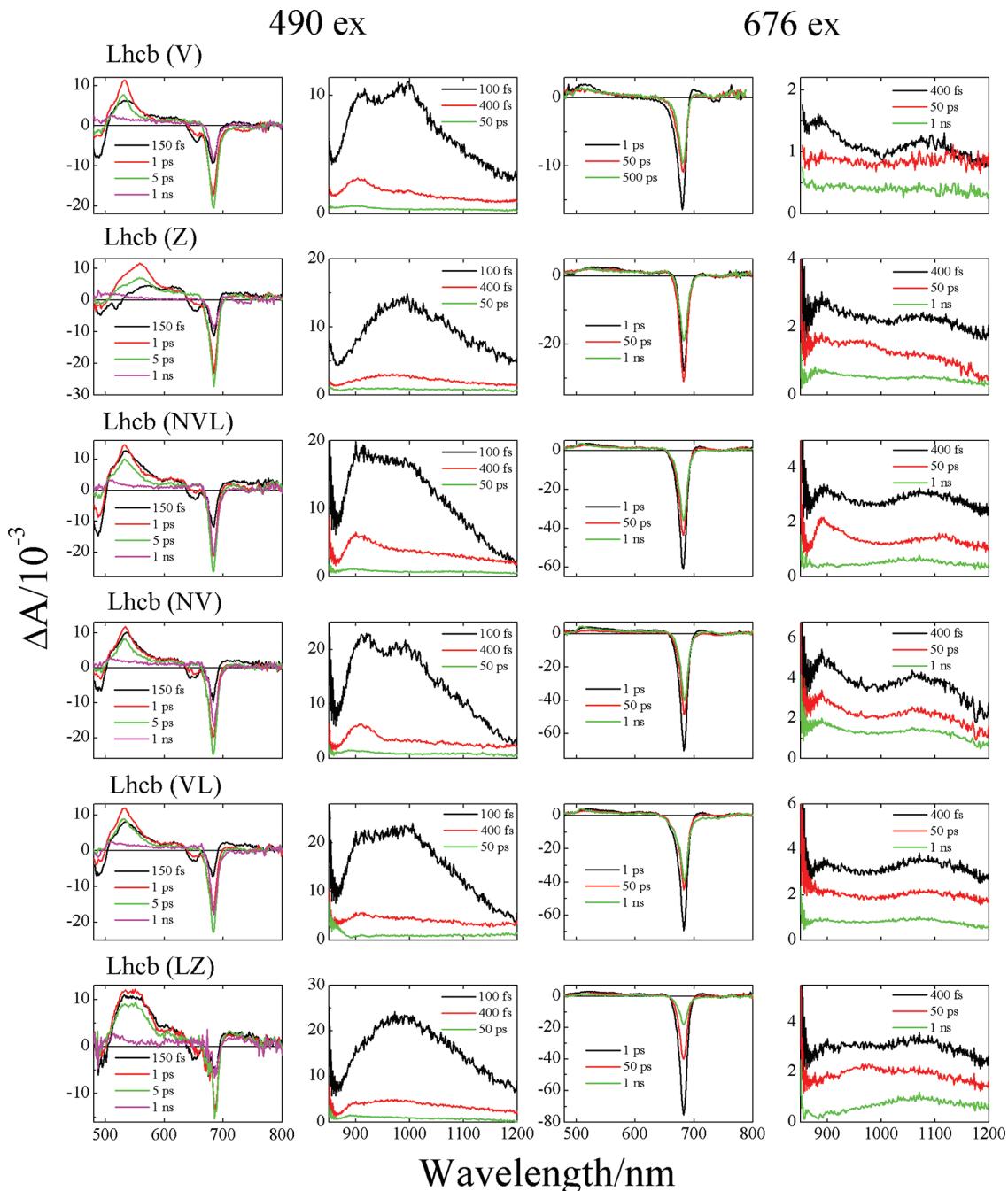


**Figure 5.** Transient absorption spectra of Lhc complexes from mutants containing V, Z, NVL (wild type), NV, VL, and LZ taken at various times (150 fs, 1 ps, 5 ps, 50 ps, and 1 ns, visible region; 100 fs, 400 fs, 50 ps, and 1 ns, NIR region) after excitation either at 490 or 676 nm.

and LHCII complexes containing Vio or Zea only (Figure 6). The absorption spectra from the complexes containing mixtures of xanthophylls were not fit due to concern over whether the resulting bandshapes would represent sufficiently unique solutions and lead to meaningful insight regarding the underlying spectral features of the pigments. Indeed, in the cases of Lhc (V), Lhc (Z), LHCII (V), and LHCII (Z), the fits given in Figure 6 should be considered as only one possible solution to this very complex deconvolution problem. However, during the course of the analysis it became clear that any reasonable fit will require at least two distinct absorption spectra for each of the protein-bound pigments to reproduce the experimental spectral lineshapes. The wavelengths of all the

Chl and xanthophyll spectral features deduced from the fits are summarized in Table 4. Because the xanthophylls most likely occupy the L1 and L2 binding sites in the protein, it is not surprising that two different absorption forms are needed. It has long been known that the absorption spectra of the two Luts that occupy the L1 and L2 sites in native LHCII are not the same.<sup>22,60</sup> However, it is surprising that the  $\lambda_{\max}$  of the absorption spectra of Vio and Zea in either the Lhc or LHCII complexes are found to differ by only 2–3 nm (Table 4). This suggests that interactions with the protein environment are more important than  $\pi$ -electron conjugation chain length in determining the energy of the  $S_0 \rightarrow S_2$  transition of protein-bound Vio and Zea. This is consistent with previous work by

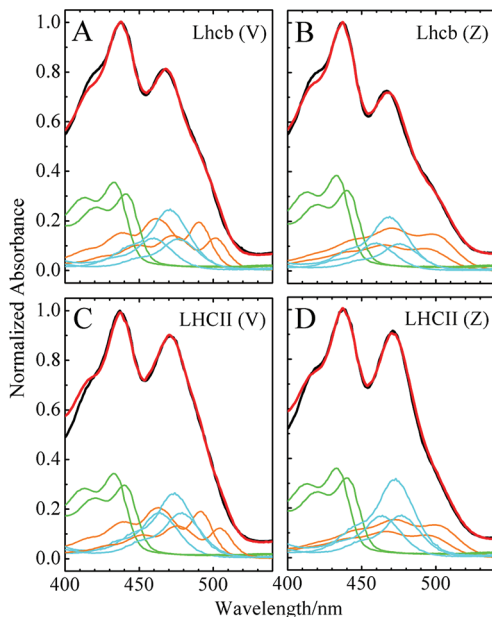


**Figure 6.** Deconvolution of the steady-state absorption spectra of LhcB (A and B) and LHCII (C and D) in the Soret and xanthophyll spectral region. The experimental spectra (black lines) were constructed (red lines) by summing the absorption spectra of the individual pigments taken in acetonitrile: Chl *a* (green lines), Chl *b* (blue lines), and xanthophylls (orange lines).

Polivka et al.<sup>61</sup> on recombinant LHCII complexes containing single xanthophylls which reported that the energies of the  $S_0 \rightarrow S_2$  transitions of protein-bound Vio and Zea differed only by  $150\text{ cm}^{-1}$  which corresponds to a spectral difference of only 4 nm in this wavelength region. The similarity in the spectra recorded here can be rationalized by assuming the protein twists the terminal  $\beta$ -ionylidine rings of Zea in a way that inhibits the extension of the  $\pi$ -electron conjugation of the polyene chain into the rings, thus rendering the spectrum of Zea similar to that of Vio whose terminal rings are not in conjugation due to the presence of epoxide groups at carbon positions 5–6 and 5'–6'.

Differences in the  $Q_y$  absorption region also become evident when one overlays and subtracts the spectra of the LhcB (V) and LHCII (V) complexes from those taken from the LhcB (Z) and LHCII (Z) complexes, respectively. A feature evident in the difference spectra shown in Figure 7 is an increase in absorption in the Chl *a* absorption region at  $\sim 685\text{ nm}$  upon changing the bound xanthophyll from Vio to Zea. This increase is accompanied by slight decreases in absorption on both sides of this feature. This behavior is evident in both the LhcB and LHCII complexes and indicates that the energy levels and spectra of at least two different Chl *a* molecules have been perturbed either by site-specific interactions with the xanthophyll or in response to the loss of Chl *b* from the protein.

Figure 7 also shows that in the  $Q_y$  region of Chl *b* absorption at  $\sim 650\text{ nm}$  the complexes containing Zea have less intensity than those containing Vio. This indicates that binding Zea to the LhcB or LHCII complex results in either the loss of a Chl *b* molecule from the pigment–protein complex or a change in oscillator strength of Chl *b* when Zea is present. A decrease in the absorption of Chl *b* was observed previously by Mozzo et al.<sup>59</sup> in LHCII trimers prepared from mutants of *Arabidopsis thaliana* containing only Lut or Lut and Zea. From the results

**Table 4. Spectral Origins ( $\lambda_{0-0}$ ) and Intensities (Measured at the  $\lambda_{\max}$ ) of the Xanthophyll and Chl Spectra Used in the Deconvolution of the Steady-State Absorption Spectra of the LhcB and LHCII Complexes Containing Exclusively Vio or Zea Shown in Figure 6**

	pigment	$\lambda_{(0-0)}/\text{nm}$	intensity
LhcB (V)	Chl <i>a</i> - 1	433	0.36
	Chl <i>a</i> - 2	441	0.31
	Chl <i>b</i> - 1	460	0.13
	Chl <i>b</i> - 2	471	0.25
	Chl <i>b</i> - 3	477	0.13
	Vio -1	490	0.19
	Vio -2	501	0.13
	Chl <i>a</i> - 1	433	0.38
	Chl <i>a</i> - 2	440	0.32
	Chl <i>b</i> - 1	460	0.11
LhcB (Z)	Chl <i>b</i> - 2	469	0.22
	Chl <i>b</i> - 3	476	0.11
	Zea -1	493	0.09
	Zea -2	498	0.15
	Chl <i>a</i> - 1	433	0.34
	Chl <i>a</i> - 2	440	0.30
	Chl <i>b</i> - 1	464	0.19
	Chl <i>b</i> - 2	474	0.27
	Chl <i>b</i> - 3	479	0.19
	Vio -1	492	0.19
LHCII (V)	Vio -2	504	0.12
	Chl <i>a</i> - 1	433	0.36
	Chl <i>a</i> - 2	440	0.32
	Chl <i>b</i> - 1	464	0.17
	Chl <i>b</i> - 2	473	0.32
	Chl <i>b</i> - 3	477	0.17
	Zea -1	494	0.09
	Zea -2	500	0.13
	LHCII (Z)		

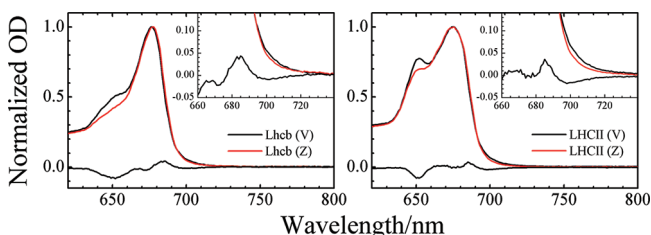


**Figure 7.** Absorption spectra in the Chl  $Q_y$  region of LhcB and LHCII complexes containing only violaxanthin or zeaxanthin along with the difference spectra obtained by subtracting the spectrum of the violaxanthin-containing complex from that of the zeaxanthin-containing complex. Inset shows an expanded plot of the difference spectra in the 660–740 nm wavelength region.

of a detailed pigment analysis, these authors found the same Chl *a*/Chl *b* ratio in the mutant complexes compared to the wild-type systems and stated that the decrease in the absorption of Chl *b* at 650 nm was typical for complexes lacking Neo. This cannot be the reason for the effect observed here since all four complexes, LhcB (V), LHCII (V), LhcB (Z), and LHCII (Z), lack Neo. HPLC analysis of the pigment content of the LHCII (NVL), LHCII (V), and LHCII (Z) complexes given in Table 2 may provide a clue to the origin of this effect. The Chl *a*/Chl *b* ratio found for LHCII (NVL) is 1.30 which, assuming there are 14 bound Chls, corresponds to 8 Chl *a* and 6 Chl *b* molecules ( $8/6 = 1.33$ ). The Chl *a*/Chl *b* ratio drops to 1.06

for LHCII (V), suggestive of the presence 7 Chl *a* and 7 Chl *b* molecules ( $7/7 = 1.00$ ), if one still assumes 14 bound Chls. In fact, this Chl *a*/Chl *b* stoichiometry is consistent with the fact that the Chl *a* Q<sub>*y*</sub> band is relatively less intense and the Chl *b* band is relatively more intense in the LHCII (V) complex compared to those of the LHCII (NVL) complex (Figure 2). The Chl *a*/Chl *b* pigment ratio increases slightly to 1.18 for LHCII (Z) (Table 2) suggestive of the presence 7 Chl *a* and 6 Chl *b* molecules ( $7/6 = 1.16$ ), i.e., the loss of a Chl pigment compared to other complexes. Once again, this Chl *a*/Chl *b* stoichiometry is consistent with the absorption spectra shown in Figure 2 in that the Chl *a* Q<sub>*y*</sub> band of LHCII (Z) is relatively more intense and the Chl *b* band is relatively less intense than those of the LHCII (V) complex. However, the Chl *a* Q<sub>*y*</sub> band of LHCII (Z) is relatively less intense and the Chl *b* band is relatively more intense than those of the LHCII (NVL) complex consistent with the difference between a 7/6 and an 8/6 Chl *a*/Chl *b* stoichiometric ratio.

To gain some insight into which protein-bound Chl molecules may be giving rise to these spectral differences, the absorption spectra from LHCII (NVL), LHCII (V), and LHCII (Z) were fit using the Chl *a* and Chl *b* spectral lineshapes in the Q<sub>*y*</sub> region obtained in the protein environment (Figure 8).<sup>57,62</sup>

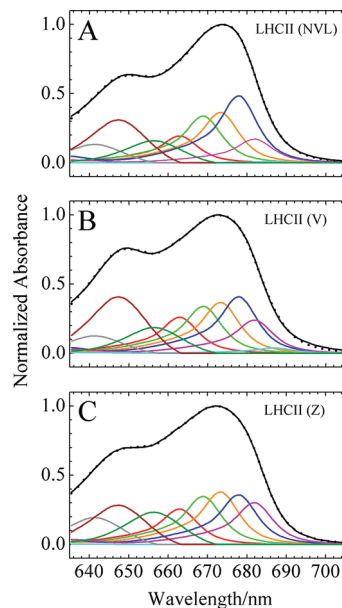


**Figure 8.** Absorption spectra of LHCII (NVL), LHCII (V), and LHCII (Z) fit using the Chl *a* and Chl *b* spectral lineshapes in the Q<sub>*y*</sub> region obtained in the protein environment.<sup>57,62</sup> The lineshapes were constructed using 5 Chl *a* and 3 Chl *b* spectral forms.<sup>63</sup>

The lineshapes were constructed using 5 Chl *a* and 3 Chl *b* spectral forms.<sup>63</sup> It can be seen in Figure 8 that upon going from LHCII (NVL) to LHCII (V) there is a decrease in the Chl *a* spectral component having a maximum at 679 nm (blue line) and an increase in the amplitude of the Chl *b* spectral component having a maximum at 649 nm (brown line). In going from LHCII (V) to LHCII (Z) there is a further reduction in the intensity of the 679 nm band, and the band at 649 nm also decreases. The spectral analysis presented in Figure 8 is actually an oversimplification of the heterogeneous nature of the spectral band shape in this wavelength region because it is very likely that the spectral bands will shift upon binding different xanthophylls. In fact, it has been shown by

mutagenesis studies that three Chl *a* molecules in sites A1, A6, and B1 (denoted Chl *a*610, *a*604, and *b*608 in the notation of Liu et al. (Figure 1)<sup>6</sup> and Chls 1, 6, and 11 in the notation of Standfuss et al.,<sup>7</sup> respectively) contribute to the absorption band at 679 nm.<sup>57</sup> These Chls are within 4.8 Å of the xanthophylls in sites L1, L2, and N1, respectively. The absorption at 649 nm is due to Chls bound in sites B3, B5, and B6 (denoted Chl *b*614, *b*609, and *b*606 in the notation of Liu et al. (Figure 1)<sup>6</sup> and Chls 8, 12, and 13 in the notation of Standfuss et al.,<sup>7</sup> respectively). Whereas the Chls in sites B3 and B5 reside nearly 8 Å from the nearest xanthophyll, the Chl *b* molecule in site B6 is 4.9 Å from the xanthophyll in site L2. The close proximity of the pigments could lead to significant shifting of the absorption bands due to changes in pigment–pigment or pigment–protein interactions when the xanthophyll composition is changed. These shifts, in addition to changes in the stoichiometry of the bound Chl *a* and *b* molecules, are likely the cause of the altered spectral bandshapes in the Q<sub>*y*</sub> region.

**Fluorescence.** The fluorescence excitation spectra shown in Figure 4 clearly indicate that Vio transfers excited state energy much more efficiently to Chl *a* than Zea. Since it is generally agreed that ~60% of the energy transfer that occurs from xanthophylls to Chls in LHCII and related minor complexes occurs from the S<sub>2</sub> state of the xanthophyll,<sup>21,22</sup> the higher efficiency in the presence of Vio must be related to stronger Coulombic coupling between its S<sub>2</sub> state and the Q<sub>*x*</sub> and Q<sub>*y*</sub> states of the Chl acceptor compared to the coupling in the presence of Zea. The change in spectral overlap cannot account for the larger efficiency of Vio because the S<sub>2</sub> energies of Vio and Zea in these complexes are rather close. It is also clear that for the complexes containing only Vio or Zea (LhcB (V), LHCII (V), LhcB (Z) and LHCII (Z)) energy transfer from Chl *b* to Chl *a* is not 100% efficient (Figure 4). However, the data also show that when Neo or Lut is present Chl *b*-to-Chl *a* transfer becomes 100% efficient. These observations can only be interpreted by differences in protein structure or electronic coupling between the Chls that arise when different xanthophylls are bound.

If one or more Chl *b* molecules are unable to transfer energy to Chl *a* when only Vio or Zea is present, then it should be the case that Chl *b* fluorescence emission is observed when the Chl *b* molecules are excited. However, fluorescence experiments carried out with 630 nm excitation (data not shown) which excites directly the Q<sub>*y*</sub> transition of Chl *b* did not reveal any emission that could be assigned to Chl *b*. This suggests that although some Chl *b* molecules may be unable to transfer energy to Chl *a* in the LhcB (V), LHCII (V), LhcB (Z), and LHCII (Z) complexes either the Chl *b* emission is too weak to be detected on the short wavelength side of the strong Chl *a* emission band or that the Chl *b* emission is quenched by the xanthophylls.

The data shown in Figure 3 and Table 3 indicate that when Zea is present in the complexes there is a decrease in both the yield and average lifetime of Chl *a* fluorescence. The differences in the fluorescence intensities seen in Figures 3A and B can be partially accounted for on the basis of the fact that energy transfer from Chl *b* to Chl *a* is not 100% efficient. However, that does not account for the differences in the intensities (Figure 3C) and lifetimes (Table 3) observed for the complexes containing solely Vio (LhcB (V) and LHCII (V)) or Zea (LhcB (Z) and LHCII (Z)) where the Chl *b*-to-Chl *a* energy transfer efficiencies are very similar (Figure 4). Note in Table 3 that in

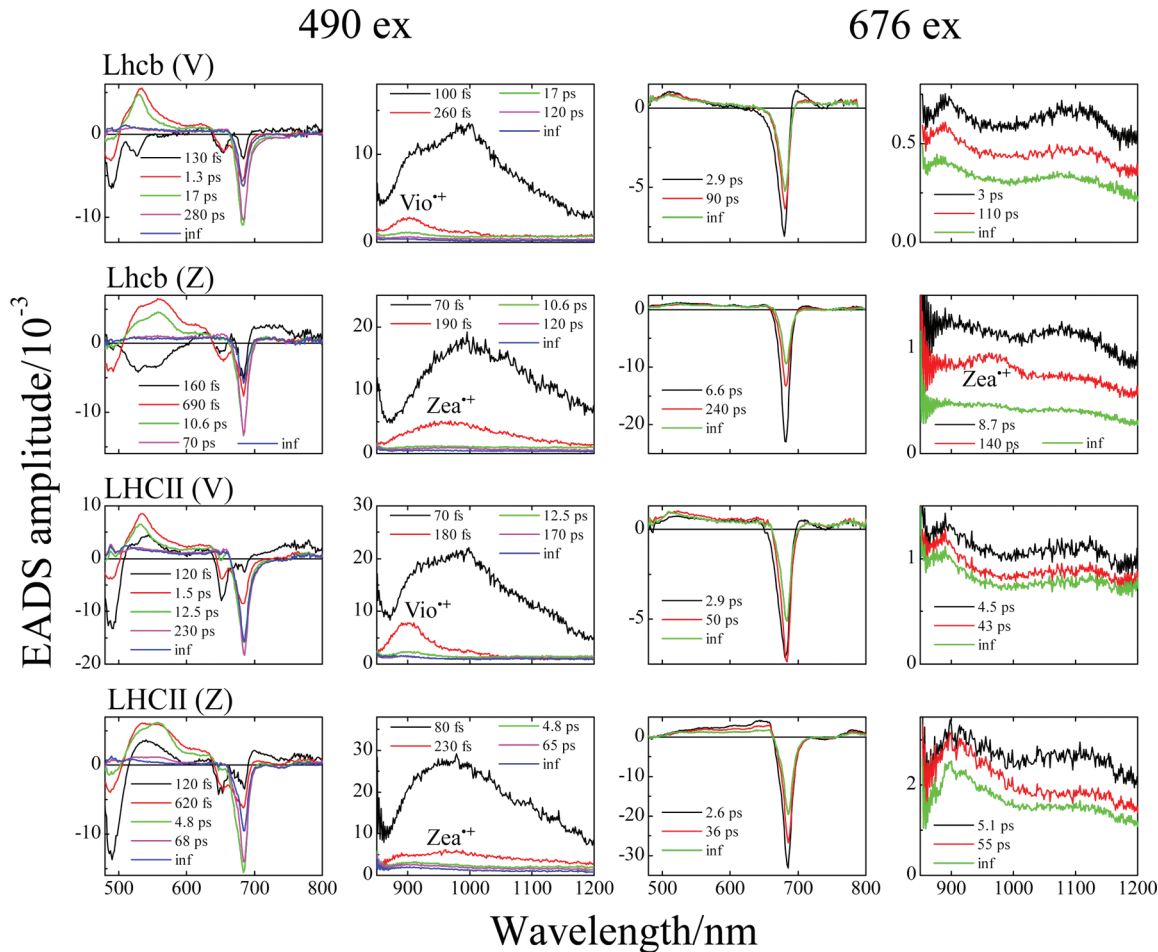


**Figure 9.** Evolution associated differential spectra of Lhc(V), Lhc(Z), LHCII(V), and LHCII(Z) at the visible and NIR spectral region, from data after 676 or 490 nm excitation. The three longest-lived components in the NIR region data set taken after 490 nm excitation were magnified by a factor of 2.

addition to a relatively large amplitude of the first fluorescence decay component from the Lhc(Z), Lhc(LZ), and LHCII(Z) complexes containing Zea the second component has a shorter lifetime compared to the analogous complexes Lhc(V), Lhc(VL), and LHCII(V) containing Vio. Accordingly, with the exception of LHCII(LZ), the results of the time-resolved fluorescence are consistent with those of the steady-state fluorescence given in Figure 3 in which the presence of Zea leads to lower levels of fluorescence from the light-harvesting complexes. The question that remains is what is the molecular mechanism for this quenching in the presence of Zea. As mentioned in the Introduction, there are several hypotheses: Energy transfer from the  $S_1$  state of Chl *a* to a low-lying xanthophyll  $S_1$  state;<sup>7,38,64</sup> the formation of a xanthophyll $^+/\text{Chl}^-$  radical pair;<sup>39</sup> exciton coupling between the  $S_1$  states of xanthophylls and Chl *a*;<sup>42</sup> and aggregation of the major LHCII pigment–protein complex.<sup>65–67</sup> For any one of these mechanisms to be considered viable, it must account for the fact that quenching is enhanced in the presence of Zea, and it must be consistent with the transient absorption experimental data.

**Global Fitting of the Transient Absorption Data Sets.** Details of the spectral changes accompanying the photo-processes that take place following excitation of the complexes can be elucidated by a global fitting analysis according to a sequential excited state decay model. The analysis yields kinetic

components and evolution associated differential spectra (EADS)<sup>68</sup> that characterize the various excited state energy transfer pathways among the bound pigments. This analysis was carried out on all of the spectral and temporal data sets, examples of which are presented in Figure 9 for the Lhc(V), Lhc(Z), LHCII(V), and LHCII(Z) complexes. The EADS traces for the rest of the complexes are provided in the Supporting Information (Figures S3 and S4), and the lifetimes of the components obtained from fits to the data sets are summarized in Table 5. Five components were required to successfully fit the spectral and temporal data sets in the region between 490 and 800 nm recorded with 490 nm excitation. The fastest component decays in  $\leq 160$  fs and has features associated with the bleaching of the  $S_0 \rightarrow S_2$  transition and stimulated emission from the  $S_2$  state of the xanthophyll as well as bleaching of the Chl *a* and *b*  $Q_Y$  bands. The absorption spectral deconvolutions given in Figure 6 show that the xanthophylls and one of the Chl *b* molecules have significant absorption at 490 nm. Since both of these pigments are excited directly by 490 nm laser light, it is difficult to distinguish which portion, if any, of the Chl *b*  $Q_Y$  band bleaching occurring at very early times is due to energy transfer from the bound xanthophylls. However, there is essentially no absorption of Chl *a* at this excitation wavelength (Figure 6). Therefore, the features in the first EADS component associated with bleaching of the  $Q_Y$  band of Chl *a* are clearly indicative of very rapid energy transfer

**Table 5. Dynamics of the Excited States of Monomeric Lhcb and LHCII Complexes<sup>a</sup>**

sample	excitation $\lambda/\text{nm}$	probe	lifetime			
			$\tau_1/\text{ps}$	$\tau_2/\text{ps}$	$\tau_3/\text{ps}$	$\tau_4/\text{ps}$
Lhcb (V)	490	vis	0.13 ± 0.05	1.3 ± 0.1	17 ± 1	280 ± 10
		NIR	<0.13	0.26 ± 0.05	17 ± 1 <sup>b</sup>	120 ± 5
Lhcb (Z)		vis	0.16 ± 0.05	0.69 ± 0.05	10.6 ± 0.4	70 ± 4
		NIR	<0.13	0.19 ± 0.05	10.6 ± 0.4 <sup>b</sup>	120 ± 5
Lhcb (NVL)		vis	<0.13	1.3 ± 0.3	11 ± 1	53 ± 4
		NIR	<0.13	1.1 ± 0.3	11 ± 1 <sup>b</sup>	53 ± 4
Lhcb (NV)		vis	<0.13	0.63 ± 0.05	8.3 ± 0.6	60 ± 5
		NIR	<0.13	0.38 ± 0.05	8.3 ± 0.6 <sup>b</sup>	100 ± 10
Lhcb (VL)		vis	<0.13	0.79 ± 0.05	9 ± 1	45 ± 4
		NIR	<0.13	0.8 ± 0.1	9 ± 1	49 ± 4
Lhcb (LZ)		vis	0.13 ± 0.05	0.69 ± 0.05	10 ± 1	75 ± 5
		NIR	<0.13	0.61 ± 0.05	10 ± 1 <sup>b</sup>	60 ± 3
LHCII (V)		vis	<0.13	1.5 ± 0.3	12.5 ± 0.7	230 ± 30
		NIR	<0.13	0.18 ± 0.05	12.5 ± 0.7 <sup>b</sup>	170 ± 10
LHCII (Z)		vis	<0.13	0.62 ± 0.05	4.8 ± 0.2	68 ± 4
		NIR	<0.13	0.23 ± 0.06	4.8 ± 0.2 <sup>b</sup>	65 ± 5
LHCII (NVL)		vis	<0.13	0.36 ± 0.05	4.5 ± 0.5	26 ± 2
		NIR	<0.13	0.50 ± 0.05	4.1 ± 0.3	22 ± 2
LHCII (NV)		vis	0.13 ± 0.05	0.84 ± 0.05	8.0 ± 0.6	63 ± 4
		NIR	<0.13	0.39 ± 0.05	8.0 ± 0.6 <sup>b</sup>	60 ± 4
LHCII (VL)		vis	0.14 ± 0.05	0.50 ± 0.05	6.6 ± 0.8	38 ± 2
		NIR	<0.13	0.48 ± 0.05	6.6 ± 0.8 <sup>b</sup>	41 ± 2
LHCII (LZ)		vis	<0.13	0.53 ± 0.05	5.0 ± 0.3	33 ± 3
		NIR	<0.13	0.50 ± 0.05	5.0 ± 0.3	63 ± 3
Lhcb (V)	676	vis	2.9 ± 0.2	90 ± 6		
		NIR	3.0 ± 0.2	110 ± 10		
Lhcb (Z)		vis	6.6 ± 0.2	240 ± 10		
		NIR	8.7 ± 0.5	140 ± 10		
Lhcb (NVL)		vis	2.6 ± 0.2	67 ± 8		
		NIR	2.8 ± 0.2	54 ± 4		
Lhcb (NV)		vis	2.6 ± 0.2	48 ± 4		
		NIR	3.0 ± 0.3	43 ± 4		
Lhcb (VL)		vis	1.9 ± 0.2	39 ± 4		
		NIR	2.8 ± 0.2	45 ± 5		
Lhcb (LZ)		vis	1.2 ± 0.1	54 ± 4		
		NIR	1.4 ± 0.1	56 ± 5		
LHCII (V)		vis	2.9 ± 0.2	50 ± 4		
		NIR	4.5 ± 0.5	43 ± 4		
LHCII (Z)		vis	2.6 ± 0.2	36 ± 2		
		NIR	5.1 ± 0.4	55 ± 5		
LHCII (NVL)		vis	0.9 ± 0.1	21 ± 1		
		NIR	0.9 ± 0.1	20 ± 2		
LHCII (NV)		vis	1.0 ± 0.2	38 ± 3		
		NIR	1.3 ± 0.3	48 ± 4		
LHCII (VL)		vis	0.50 ± 0.05	18 ± 2		
		NIR	3.8 ± 0.4	62 ± 4		
LHCII (LZ)		vis	0.60 ± 0.06	30 ± 2		
		NIR	1.1 ± 0.5	56 ± 8		

<sup>a</sup>The values were derived from global analysis. The uncertainties in the numbers were determined from an examination of the region of solution for each fitted parameter based on the values of the residuals. In addition to the lifetimes below, a final infinite component is assigned in the global analysis of all complexes. <sup>b</sup>Lifetime fixed according to the S<sub>1</sub>–S<sub>N</sub> component from the visible data sets.

to Chl *a* from either the S<sub>2</sub> state of the photoexcited xanthophylls or from Chl *b*.

In going from the initial EADS component which decays in ≤160 fs to the second EADS component, there is a decrease in the bleaching of the S<sub>0</sub> → S<sub>2</sub> transition of the xanthophylls around 495 nm and an increase in the bleaching of the Chl *a* Q<sub>Y</sub> absorption band. However, no additional increase in the

bleaching of the Chl *b* Q<sub>Y</sub> absorption is evident. This indicates that no energy transfer from the xanthophylls to Chl *b* is taking place in this time range but that energy transfer to Chl *a*, presumably from the S<sub>2</sub> state of the xanthophylls, is proceeding. This second EADS component also shows a broad positive feature between 500 and 600 nm that can be attributed to a vibronically hot S<sub>1</sub> → S<sub>N</sub> transition of the xanthophylls. The

appearance of this band indicates that the  $S_1$  state of the xanthophylls is being populated by deactivation of the  $S_2$  state in  $\leq 160$  fs. Also, this feature is much broader for the samples containing Zea than it is for the samples containing Vio due to enhanced conformational disorder which is also evident in the steady-state absorption bands of these xanthophylls (Figure 6). The broad positive feature decreases in amplitude and narrows as the second EADS component decays in 0.5–1.5 ps to form the third EADS component. This decrease in amplitude and narrowing is accompanied by the disappearance of the bleaching of the Chl *b*  $Q_y$  band and a further increase in the bleaching of the Chl *a*  $Q_y$  band. This suggests, and it has been shown from previous studies,<sup>69</sup> that this process is due to a combination of relaxation of the vibrationally hot  $S_1$  state of the xanthophylls which narrows the  $S_1 \rightarrow S_N$  transition and energy transfer from the xanthophylls and Chl *b* to Chl *a*. The line shape of this third EADS component is dominated by the characteristic  $S_1 \rightarrow S_N$  excited state absorption of the xanthophylls and bleaching of the  $Q_y$  band of Chl *a*. In going from the third to the fourth EADS component, there is a complete disappearance of the positive amplitude attributable to the  $S_1 \rightarrow S_N$  excited state absorption of the xanthophylls without any measurable increase in the amplitude associated with the bleaching of the  $Q_y$  band of Chl *a*. This indicates that the  $S_1$  state of the xanthophylls is only minimally involved, if at all, in transferring energy to Chl *a* in accord with previous work on native LHCII complexes.<sup>22</sup> Thus, the third EADS component which has a lifetime in the range 4.8–17.5 ps represents the  $S_1$  state lifetime of the protein-bound xanthophylls largely unaffected by energy transfer to Chl *a*. The fourth EADS component has a lifetime between 33 and 300 ps that decays into a final infinitely long (for this experiment) component. This decay is characterized by a decrease in the bleaching of the  $Q_y$  band of Chl *a* and the appearance of a small positive feature between 510 and 550 nm. It is obvious that the maxima of these weak bands do not match the  $S_1 \rightarrow S_N$  maxima, which are located at 530 and 550 nm, respectively, indicating that this amplitude can not be attributed to the  $S_1$  state of xanthophylls populated by back transfer from the  $S_1$  state of Chl *a*.<sup>38</sup> Instead, the peaks at 510 and 525 nm are comparable to the known maxima of xanthophyll triplet state absorption bands,<sup>59</sup> suggesting that the slow process may be attributable to the formation of xanthophyll triplet states.

In going from the fourth to the final EADS component in the global fitting analysis of the visible region data sets taken using 490 nm excitation, the observed decrease in the bleaching of the Chl *a*  $Q_y$  band indicates that some Chl *a* excited state population is returning to the ground state. If this is due to the formation of Chl *a* triplet states which are then rapidly quenched by xanthophyll triplets, the same (infinite) component should be evident in the EADS analysis of the data sets taken using 676 nm light that directly excites Chl *a*. Figure 10 overlays the final EADS components resulting from analysis of the data sets taken using excitation at the two different wavelengths (490 and 676 nm). The agreement between the traces is very good for the samples containing Vio and supports the assignment of this photoprocess to triplet state formation. For Zea-containing samples, the agreement is less obvious, but the band located at 525 nm is present in both 490 and 676 nm excitation, supporting the assignment of the bands as due to triplet states of xanthophylls.

The kinetic data reveal that the complexes containing Vio have longer  $S_1$  state lifetimes (17.5 ps for Lhcb (V) and 12.5 ps

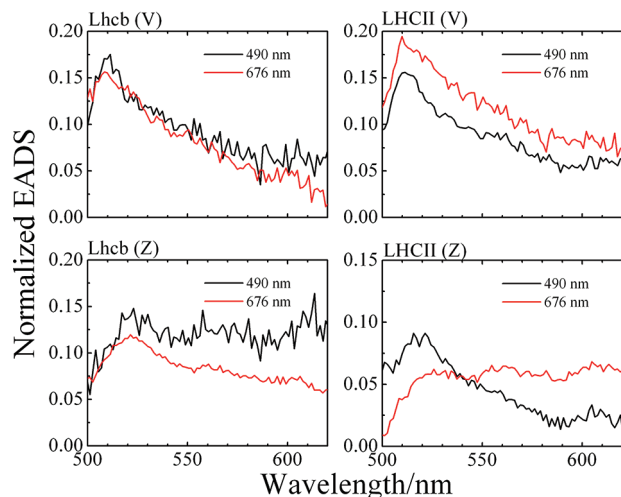


**Figure 10.** Overlay of the final EADS components shown in Figure 9 taken using 490 and 676 nm excitation.

for LHCII(V)) than those containing Zea (10.6 ps for Lhcb (Z) and 4.8 ps LHCII (Z)). These values compare with the  $S_1$  lifetimes of these xanthophylls in solution which are 24 ps for Vio and 9 ps for Zea.<sup>64,70</sup> Also, except for Zea in the Lhcb (Z) complex, the lifetimes observed for the xanthophylls in the complexes are shorter than those measured in solution which suggests the  $S_1$  state as a route of energy transfer to Chl. However, as noted above, the disappearance of the  $S_1 \rightarrow S_N$  transition in going from the third to the fourth EADS component is not accompanied by an increase in the bleaching of the Chl *a*  $Q_y$  band. Therefore, energy transfer to Chl cannot be the explanation for the shorter lifetimes of the xanthophylls in the protein compared to their values in solution. The data can only be rationalized by assuming that upon binding to the protein the properties of the  $S_1$  state of the xanthophylls are altered in such a way that enhances their rate of deactivation to the ground state. This is the same conclusion reached previously by Polivka et al.<sup>61</sup> based on similar experiments on recombinant LHCII complexes containing these same xanthophylls. In those experiments, however, both Zea and Vio exhibited nearly identical lifetimes of 11 ps in LHCII complexes prepared by refolding in vitro the LHCII apoprotein with either Vio or Zea.<sup>61</sup> Because different results are obtained here, it clearly suggests that the spectroscopic properties of xanthophylls in LHCII are very sensitive to the local protein environment.

The NIR data sets taken using 490 nm excitation also required five components for a good fit (Figure 9). The fastest EADS component has a broad positive band that can be attributed to  $S_2 \rightarrow S_N$  excited state absorption, but the spectrum in this region also displays a feature on the short wavelength side of the broad band. As the first EADS component decays in  $\leq 100$  fs to form the second EADS component, a clear positive band is evident at  $\sim 910$  nm for the samples containing Vio (Lhcb (V) and LHCII (V)). This band is broader and red-shifted to  $\sim 960$  nm for the samples containing Zea (Lhcb (Z) and LHCII (Z)). The amplitude profiles of these EADS components are very similar to the NIR spectra of radical cations of Vio<sup>•+</sup> and Zea<sup>•+</sup> and therefore can be assigned to these species.<sup>71</sup> In fact, the wavelengths of these bands are very similar to those reported by Wachtveitl et al.<sup>72,73</sup> and assigned to radical cations. In that work the spectra of the

Vio and Zea cations have comparable linewidths, while in our case the Vio radical cation signal is significantly narrower than that of Zea. Previous work by us examining the steady-state absorption spectra of the radical cations of Vio and Zea in solution clearly shows that the Vio radical cation spectrum is significantly narrower than that of Zea.<sup>71</sup> Moreover, the ~60 nm line width of the radical cation spectrum of Vio in the complexes is in very good agreement with that observed for Vio in solution. This suggests that the current samples are slightly different from those analyzed by Wachtveitl et al. The features associated with the radical cations decay in 190–260 fs to form the third EADS component which has very weak positive amplitude that can be assigned to a combination of radical cation species and  $S_1 \rightarrow S_2$  excited state absorption bands of the xanthophylls. This third component decays in 4.8–17.5 ps which is expected based on the lifetimes of the  $S_1$  states of the xanthophylls to form a fourth component which has very weak positive features and a lifetime between 65 and 170 ps. This amplitude and that of the infinite component are too weak to make a compelling argument for their assignment.

Transient absorption spectra recorded in the visible region using 676 nm excitation which directly excites the Chl *a*  $Q_y$  band were able to be fit using only three components. As the first component decays into the second component in a time between 2.6 and 6.4 ps, there is a decrease in the bleaching of the Chl *a*  $Q_y$  band. This is due to Chl *a* excitation annihilation because it shows a clear dependence on the intensity of the excitation pulse. Figure 11 shows a fit of the transient

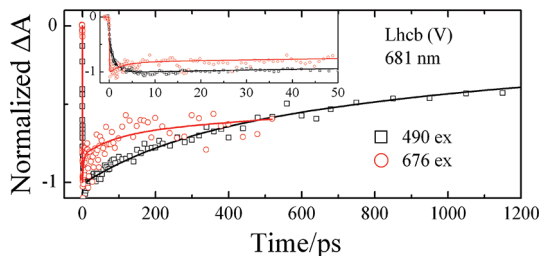


**Figure 11.** Normalized kinetic traces of Lhcb (V) (A) taken at 681 nm after excitation at 490 nm (black squares) and 676 nm (red circles). Lines represent fits from global analysis. Panel B shows kinetic traces of Lhcb (V) taken at 681 nm after excitation at 676 nm with varying pulse energy. The intensity values are in units of photons/cm<sup>2</sup> pulse.

absorption kinetic response at 681 nm from the Lhcb (V) complex excited at 490 and 676 nm. The inset in the figure shows a slow (~10 ps) rise in the kinetics taken upon 490 nm excitation which is then followed by an even slower decay. The kinetics probed after excitation at 676 nm shows a fast decay (~5 ps) followed by slower decay components. The dependence of this fast decay on laser pump intensity (data not shown) indicates that it is due to exciton annihilation. Interestingly, annihilation was only observed when Chl *a* molecules were directly excited at 676 nm. No evidence of annihilation was observed when 490 nm excitation was used (Figure 11). This suggests that the various Chl *a* molecules in the protein that become excited by energy transfer either from the xanthophylls or from Chl *b* reside in distant binding sites which make them less prone to encounter each other and annihilate compared to those that are populated by direct excitation of the Chl *a*  $Q_y$  transition. As the second component decays to form the third (infinitely long) component, there is a further decrease in the bleaching of the Chl *a*  $Q_y$  band which

may be attributable to the formation of Chl *a* triplet states which are quenched by xanthophyll triplets as mentioned above.

Note from the data presented in Figures 5 and 9 and Figure S2 (Supporting Information) that upon direct excitation of the xanthophylls at 490 nm absorption bands associated with the formation of Vio and Zea radical cations are clearly seen in the NIR (red traces in the second column of Figure 9). The bands appear at ~910 nm for Vio<sup>•+</sup> and at ~990 nm for Zea<sup>•+</sup>. Also, upon excitation of the Chl  $Q_y$  band at 676 nm, Lhcb (Z) (red trace in the second row, last column panel of Figure 9) shows a clear band attributable to Zea<sup>•+</sup> at ~990 nm. This feature is not observed in the Lhcb (V) sample nor in any of the LHCII samples (Figure 9 and Figures S4, Supporting Information). However, the feature is seen in the EADS of the Lhcb (LZ) sample excited at 676 nm (red trace in the last row, last column panel of Figure S3, Supporting Information). Moreover, the time constants for the formation (8.7 ps) and decay (140 ps) of the Zea<sup>•+</sup> radical cation in the Lhcb (Z) sample are very similar to those reported by Avenson et al.<sup>74</sup> These observations confirm that the formation of a xanthophyll radical cation upon Chl excitation requires the presence of Zea in a minor antenna complex of PSII.

One remaining issue is to reconcile the steady-state fluorescence excitation spectra of the Lhcb (V and Z) and LHCII (V and Z) complexes which show that Chl *b*-to-Chl *a* energy transfer is not 100% (Figure 4), with the transient absorption data in Figures 5 and 9 and Figure S2 (Supporting Information) which do not show residual (nanosecond-long) bleaching of the Chl *b*  $Q_y$  band in any of the spectral traces. One would expect that if there are Chl *b* molecules in these complexes incapable of transferring energy to Chl *a* there should be evidence of this in the form of long-lived bleaching in the region of the Chl *b*  $Q_y$  absorption band. One possibility is that 490 nm excitation does not excite Chl *b* at all and that the bleaching of the Chl *b*  $Q_y$  band derives entirely from very rapid energy transfer from the xanthophylls. As noted above, this is unlikely due to the fact that the spectral deconvolution shown in Figure 6 indicates that at least one of the spectral forms of Chl *b* has a tailing absorption of its Soret band at this wavelength. Previous reports have also suggested this to be the case for Chl *b*.<sup>61</sup> However, the absence of residual Chl *b* bleaching can be rationalized if two different spectral forms of Chl *b* molecules are present as suggested by the spectral deconvolution shown in Figure 6. The first spectral form would be excited by 490 nm light, rapidly bleached in the  $Q_y$  absorption region, and capable of transferring energy to Chl *a*. The other blue-shifted spectral form would not be excited by 490 nm light, not exhibit bleaching of its  $Q_y$  band, not be able to transfer energy to Chl *a*, and therefore not sensitize Chl *a* fluorescence in an excitation scan through the Chl *b*  $Q_y$  absorption region (Figure 4).

## CONCLUSIONS

The data taken here on the various LHCII and Lhcb complexes prepared from *Arabidopsis thaliana* mutant plants confirm previous observations that energy transfer from xanthophylls to Chl *a* is not 100% efficient. In addition, the data clearly show that energy transfer from Zea to Chl *a* is much less efficient than from Vio to Chl *a*. In the complexes containing Vio or Zea as sole xanthophylls, some Chl *b* molecules are not able to transfer energy to Chl *a*. These results suggest that varying the xanthophyll composition induces small structural changes that

affect the interaction between pigments and lead to alterations in energy transfer efficiencies as a means of regulating energy flow within the complexes. Also, the complexes containing Zea exhibit lower yields and shorter lifetimes of Chl *a* fluorescence than those containing Vio. The effect cannot be attributed to aggregation of the (monomeric) complexes studied here, but radical cation formation in the minor Lhcb complexes containing Zea may play a role. Exciton interactions between the bound Zeas and Chl *a* cannot be ruled out as a quenching pathway, however, and neither can the mechanism whereby the excited S<sub>1</sub> state of Chl *a* transfers energy to the S<sub>1</sub> state of Zea. However, no evidence for this type of energy transfer is observed, nor is it expected to be readily observed due to the nanosecond time scale for the transfer compared to the picosecond time scale for the deactivation of the Zea S<sub>1</sub> state. These distinct dynamics would lead to a very small S<sub>1</sub> excited state population for Zea that would be difficult to detect in a transient absorption experiment probing the S<sub>1</sub> → S<sub>N</sub> transition. Nevertheless, Zea and Vio triplet states are generated on a time scale of hundreds of picoseconds, and these are observed to lead to a reduction in the population of Chl *a* excited states.

## ASSOCIATED CONTENT

### Supporting Information

SDS-PAGE analyses of the polypeptide composition of Lhcb and LHCII complexes, percentage of antenna proteins in the samples, transient absorption spectra of LHCII complexes from mutants containing V, N, NVL (wild type), NV, VL, and LZ in the visible and NIR spectral region after 676 or 490 nm excitation, and evolution associated differential spectra of Lhcb and LHCII complexes from mutants containing NVL, NV, VL, and LZ in the visible and NIR spectral region after 676 or 490 nm excitation. This material is available free of charge via the Internet at <http://pubs.acs.org>.

## AUTHOR INFORMATION

### Notes

The authors declare no competing financial interest.

## ACKNOWLEDGMENTS

Work in the laboratory of HAF was supported by grants from the National Science Foundation (MCB-0913022) and the University of Connecticut Research Foundation. Work in the laboratory of R.B. was supported by the Italian Ministry of Research (Programmi di Ricerca di Interesse Nazionale PRIN No. 2008XB774B) and by EU project PITN-GA-2009-238017 1030 HARVEST. T.P. thanks the Czech Ministry of Education for financial support (Grant No. ME09037).

## REFERENCES

- (1) Jansson, S. *Trends Plant Sci.* **1999**, *4*, 236.
- (2) Green, B. R.; Parson, W. W. *Light-Harvesting Antennas in Photosynthesis*; Kluwer Academic Publishers: Dordrecht, 2003; Vol. 13.
- (3) Niyogi, K. K.; Grossman, A. R.; Björkman, O. *Plant Cell* **1998**, *10*, 1121.
- (4) Peter, G. F.; Thornber, J. P. *J. Biol. Chem.* **1991**, *266*, 16745.
- (5) Caffari, S.; Croce, R.; Breton, J.; Bassi, R. *J. Biol. Chem.* **2001**, *276*, 35924.
- (6) Liu, Z. F.; Yan, H. C.; Wang, K. B.; Kuang, T. Y.; Zhang, J. P.; Gui, L. L.; An, X. M.; Chang, W. R. *Nature* **2004**, *428*, 287.
- (7) Standfuss, J.; van Scheltinga, A. C. T.; Lamborghini, M.; Küllbrandt, W. *EMBO J.* **2005**, *24*, 919.
- (8) Takaichi, S.; Mimuro, M. *Plant Cell Physiol.* **1998**, *39*, 968.
- (9) Croce, R.; Weiss, S.; Bassi, R. *J. Biol. Chem.* **1999**, *274*, 29613.
- (10) Hobe, S.; Niemeier, H.; Bender, A.; Paulsen, H. *Eur. J. Biochem.* **2000**, *267*, 616.
- (11) Yamamoto, H. Y. *Methods Enzymol.* **1985**, *110*, 303.
- (12) Demmig-Adams, B. *Biochim. Biophys. Acta* **1990**, *1020*, 1.
- (13) Bassi, R.; Pineau, B.; Dainese, P.; Marquardt, J. *Eur. J. Biochem.* **1993**, *212*, 297.
- (14) Hankamer, B.; Barber, J.; Boekema, E. J. *Annual Rev. Plant Physiol. Plant Mol. Biol.* **1997**, *48*, 641.
- (15) Harrer, R.; Bassi, R.; Testi, M. G.; Schafer, C. *Eur. J. Biochem.* **1998**, *255*, 196.
- (16) Boekema, E. J.; Van Roon, H.; Calkoen, F.; Bassi, R.; Dekker, J. P. *Biochemistry* **1999**, *38*, 2233.
- (17) Das, S. K.; Frank, H. A. *Biochemistry* **2002**, *41*, 13087.
- (18) Pan, X.; Li, M.; Wan, T.; Wang, L.; Jia, C.; Hou, Z.; Zhao, X.; Zhang, J.; Chang, W. *Nat. Struct. Mol. Biol.* **2011**, *18*, 309.
- (19) Connelly, J. P.; Mueller, M. G.; Bassi, R.; Croce, R.; Holzwarth, A. R. *Biochemistry* **1997**, *36*, 281.
- (20) Peterman, E. J. G.; Monshouwer, R.; van Stokkum, I. H. M.; van Grondelle, R.; van Amerongen, H. *Chem. Phys. Lett.* **1997**, *264*, 279.
- (21) Grdinaru, C. C.; van Stokkum, I. H. M.; Pascal, A. A.; van Grondelle, R.; van Amerongen, H. *J. Phys. Chem. B* **2000**, *104*, 9330.
- (22) Croce, R.; Muller, M. G.; Bassi, R.; Holzwarth, A. R. *Biophys. J.* **2001**, *80*, 901.
- (23) Walla, P. J.; Linden, P. A.; Ohta, K.; Fleming, G. R. *J. Phys. Chem. A* **2002**, *106*, 1909.
- (24) Croce, R.; Muller, M. G.; Caffari, S.; Bassi, R.; Holzwarth, A. R. *Biophys. J.* **2003**, *84*, 2517.
- (25) Akimoto, S.; Yokono, M.; Ohmae, M.; Yamazaki, I.; Tanaka, A.; Higuchi, M.; Tsuchiya, T.; Miyashita, H.; Mimuro, M. *J. Phys. Chem. B* **2005**, *109*, 12612.
- (26) Hudson, B.; Kohler, B. *Annu. Rev. Phys. Chem.* **1974**, *25*, 437.
- (27) Christensen, R. L.; Barney, E. A.; Broene, R. D.; Galinato, M. G. I.; Frank, H. A. *Arch. Biochem. Biophys.* **2004**, *430*, 30.
- (28) Kwa, S. L. S.; Van Amerongen, H.; Lin, S.; Dekker, J. P.; Van Grondelle, R.; Struve, W. S. *Biochim. Biophys. Acta* **1992**, *1102*, 202.
- (29) Bittner, T.; Irrgang, K. D.; Renger, G.; Wasilewski, M. R. *J. Phys. Chem.* **1994**, *98*, 11821.
- (30) Connelly, J. P.; Müller, M. G.; Hucke, M.; Gatzen, G.; Mullineaux, C. W.; Ruban, A. V.; Horton, P.; Holzwarth, A. R. *J. Phys. Chem. B* **1997**, *101*, 1902.
- (31) Grdinaru, C. C.; Van Stokkum, I. H. M.; Van Grondelle, R.; Van Amerongen, H. *Photosynthesis: Mechanisms and Effects, Proceedings of the International Congress on Photosynthesis*, 11th, Budapest, Aug. 17–22, 1998; Vol. 1, p 277.
- (32) Agarwal, R.; Krueger, B. P.; Scholes, G. D.; Yang, M.; Yom, J.; Mets, L.; Fleming, G. R. *J. Phys. Chem. B* **2000**, *104*, 2908.
- (33) van Amerongen, H.; van Grondelle, R. *J. Phys. Chem. B* **2001**, *105*, 604.
- (34) Holt, N. E.; Kennis, J. T. M.; Dall'Osto, L.; Bassi, R.; Fleming, G. R. *Chem. Phys. Lett.* **2003**, *379*, 305.
- (35) Cheng, Y.-C.; Ahn, T.-K.; Avenson, T. J.; Zigmantas, D.; Niyogi, K. K.; Ballottari, M.; Bassi, R.; Fleming, G. R. *J. Phys. Chem. B* **2008**, *112*, 13418.
- (36) Polívka, T.; Frank, H. A. *Acc. Chem. Res.* **2010**, *43*, 1125.
- (37) Pascal, A. A.; Liu, Z.; Broess, K.; van Oort, B.; van Amerongen, H.; Wang, C.; Horton, P.; Robert, B.; Chang, W.; Ruban, A. V. *Nature* **2005**, *436*, 134.
- (38) Ruban, A. V.; Berera, R.; Illoiaia, C.; van Stokkum, I. H. M.; Kennis, J. T. M.; Pascal, A. A.; van Amerongen, H.; Robert, B.; Horton, P.; van Grondelle, R. *Nature* **2007**, *450*, 575.
- (39) Holt, N. E.; Zigmantas, D.; Valkunas, L.; Li, X. P.; Niyogi, K. K.; Fleming, G. R. *Science* **2005**, *307*, 433.
- (40) Ahn, T. K.; Avenson, T. J.; Ballottari, M.; Cheng, Y. C.; Niyogi, K. K.; Bassi, R.; Fleming, G. R. *Science* **2008**, *320*, 794.
- (41) Bode, S.; Quentmeier, C. C.; Liao, P.-N.; Barros, T.; Walla, P. J. *Chem. Phys. Lett.* **2008**, *450*, 379.

- (42) Bode, S.; Quentmeier, C. C.; Liao, P.-N.; Hafi, N.; Barros, T.; Wilk, L.; Bittner, F.; Walla, P. J. *Proc. Natl. Acad. Sci. U.S.A.* **2009**, *106*, 12311.
- (43) Liao, P. N.; Bode, S.; Wilk, L.; Hafi, N.; Walla, P. J. *Chem. Phys.* **2010**, *373*, 50.
- (44) Miloslavina, Y.; Wehner, A.; Lambrev, P. H.; Wientjes, E.; Reus, M.; Garab, G.; Croce, R.; Holzwarth, A. R. *FEBS Lett.* **2008**, *582*, 3625.
- (45) Holzwarth, A. R.; Miloslavina, Y.; Nilkens, M.; Jahns, P. *Chem. Phys. Lett.* **2009**, *483*, 262.
- (46) Muller, M. G.; Lambrev, P.; Reus, M.; Wientjes, E.; Croce, R.; Holzwarth, A. R. *ChemPhysChem* **2010**, *11*, 1289.
- (47) DellaPenna, D. *Pure Appl. Chem.* **1999**, *71*, 2205.
- (48) Dall'Osto, L.; Caffarri, S.; Bassi, R. *Plant Cell* **2005**, *17*, 1217.
- (49) Sakuraba, Y.; Tanaka, R.; Yamasato, A.; Tanaka, A. *J. Biol. Chem.* **2009**, *284*, 36689.
- (50) Dall'Osto, L.; Fiore, A.; Cazzaniga, S.; Giuliano, G.; Bassi, R. *J. Biol. Chem.* **2007**, *282*, 35056.
- (51) Mathies, G.; van Hemert, M. C.; Gast, P.; Gupta, K.; Frank, H. A.; Lugtenburg, J.; Groenen, E. J. *J. Phys. Chem. A* **2011**, *115*, 9552.
- (52) Dainese, P.; Hoyer-Hansen, G.; Bassi, R. *Photochem. Photobiol.* **1990**, *51*, 693.
- (53) Gilmore, A. M.; Yamamoto, H. Y. *Plant Physiol.* **1991**, *96*, 635.
- (54) Ilagan, R. P.; Christensen, R. L.; Chapp, T. W.; Gibson, G. N.; Pascher, T.; Polívka, T.; Frank, H. A. *J. Phys. Chem. A* **2005**, *109*, 3120.
- (55) Dall'Osto, L.; Cazzangia, S.; North, H.; Marion-Poll, A.; Bassi, R. *Plant Cell* **2007**, *19*, 1048.
- (56) Bassi, R.; Croce, R.; Cugini, D.; Sandona, D. *Proc. Natl. Acad. Sci. U.S.A.* **1999**, *96*, 10056.
- (57) Remelli, R.; Varotto, C.; Sandona, D.; Croce, R.; Bassi, R. *J. Biol. Chem.* **1999**, *274*, 33510.
- (58) Croce, R.; Canino, G.; Ros, F.; Bassi, R. *Biochemistry* **2002**, *41*, 7334.
- (59) Mozzo, M.; Dall'Osto, L.; Hienerwadel, R.; Bassi, R.; Croce, R. *J. Biol. Chem.* **2008**, *283*, 6184.
- (60) Croce, R.; Cinque, G.; Holzwarth, A. R.; Bassi, R. *Photosynth. Res.* **2000**, *64*, 221.
- (61) Polívka, T.; Zigmantas, D.; Sundström, V.; Formaggio, E.; Cinque, G.; Bassi, R. *Biochemistry* **2002**, *41*, 439.
- (62) Cinque, G.; Croce, R.; Bassi, R. *Photosynth. Res.* **2000**, *64*, 233.
- (63) Caffarri, S.; Croce, R.; Cattivelli, L.; Bassi, R. *Biochemistry* **2004**, *43*, 9467.
- (64) Frank, H. A.; Cua, A.; Chynwat, V.; Young, A.; Gosztola, D.; Wasielewski, M. R. *Photosynth. Res.* **1994**, *41*, 389.
- (65) Horton, P.; Ruban, A. V.; Rees, D.; Pascal, A. A.; Noctor, G.; Young, A. J. *FEBS Lett.* **1991**, *292*, 1.
- (66) Ruban, A. V.; Rees, D.; Pascal, A. A.; Horton, P. *Biochim. Biophys. Acta* **1992**, *1102*, 39.
- (67) Mullineaux, C. W.; Pascal, A. A.; Horton, P.; Holzwarth, A. R. *Biochim. Biophys. Acta* **1993**, *1141*, 23.
- (68) van Stokkum, I. H. M.; Larsen, D. S.; van Grondelle, R. *Biochim. Biophys. Acta* **2004**, *1657*, 82.
- (69) Billsten, H. H.; Zigmantas, D.; Sundström, V.; Polívka, T. *Chem. Phys. Lett.* **2002**, *355*, 465.
- (70) Polívka, T.; Herek, J. L.; Zigmantas, D.; Åkerlund, H. E.; Sundström, V. *Proc. Natl. Acad. Sci. U.S.A.* **1999**, *96*, 4914.
- (71) Galinato, M. G. I.; Niedzwiedzki, D.; Deal, C.; Birge, R. R.; Frank, H. A. *Photosynth. Res.* **2007**, *94*, 67.
- (72) Amarie, S.; Standfuss, J.; Barros, T.; Kühlbrandt, W.; Dreuw, A.; Wachtveitl, J. *J. Phys. Chem. B* **2007**, *111*, 3481.
- (73) Amarie, S.; Wilk, L.; Barros, T.; Kühlbrandt, W.; Dreuw, A.; Wachtveitl, J. *Biochim. Biophys. Acta* **2009**, *1787*, 747.
- (74) Avenson, T. J.; Ahn, T. K.; Zigmantas, D.; Niyogi, K.; Li, Z.; Ballottari, M.; Bassi, R.; Fleming, G. R. *J. Biol. Chem.* **2008**, *283*, 3550.